Hindawi
International Journal of RF and Microwave Computer-Aided Engineering
Volume 2023, Article ID 3110383, 22 pages
https://doi.org/10.1155/2023/3110383

Research Article

New Multipriority and Variable Duration Triple Time Slot P-CSMA Protocol for Edge Servers Server Deployment

Hongwei Ding,[1] **Wenmin Pei**,[1] **Yongtao Yu**,[2] **Peng Hu**,[3] **Bo Li**,[1] **and Xu Lu**[1]

[1]*School of Information Science and Engineering, Yunnan University, Kunming 650500, China*
[2]*Yunnan Key Laboratory of Smart City and Cyberspace Security, Yuxi 653100, China*
[3]*Research and Development Department, Youbei Technology Company, LTD, Kunming 650000, China*

Correspondence should be addressed to Yongtao Yu; tomaloha@qq.com

Received 25 February 2023; Revised 25 April 2023; Accepted 9 May 2023; Published 25 May 2023

Academic Editor: Mangal Sain

In this paper, we study the joint impact of task priority and transmission time slot variable computing services on a novel p-persistent random multiple access communication protocol (p-persistent CSMA) in an edge server network. The traditional p-persistent CSMA protocol performs better at low loads, and in order to make the protocol perform better even when the edge server network is accessed by a large number of smart terminals, we consider adding a variable success time slot length and a multichannel, multipriority access model. When the success time slot is longer, the nodes will take longer time to send data, which will reduce the number of nodes retransmitting data, thus improving channel utilization and making the throughput rate of the network increase accordingly. Then, different priority levels are assigned according to the user's needs, and the higher the priority level, the more channels are occupied and the probability of successful message delivery increases. Finally, the superiority of the proposed protocol is verified by simulation.

1. Introduction

In recent years, with the proposal of edge computing, a large number of end devices have been connected to the network with the help of edge servers [1]. The edge server is the core device of edge computing, which provides a channel for multiple users to enter the network to communicate with the devices in other servers. However, when multiple end devices access the same edge server at the same time, information collision may occur resulting in communication failure. In order that different end devices can be connected more efficiently in the network, continuous improvement of multi-access communication techniques in edge server networks has become a hot topic of current research [2].

Multiple access technologies are divided into three main categories: fixed-assignment multiple access, multiple access on demand, and random multiple access [3]. Common fixed-assignment multiple accesses include frequency division multiple access (FDMA), time division multiple access (TDMA), and code division multiple access (CDMA), which are fixed-assignment, so the transmission rate of the channel is easily limited and the requirements for the base station are high. On-demand multiple access allocates bandwidth according to the length of data that the user needs to send, which may lead to increased transmission delays and thus affect communication quality since channel allocation needs to be performed before transmission. Both of the above protocols are noncompetitive, and they are less capable of handling strongly bursty services. Thus the random multiple access technique (CSMA) was born, which was proposed to solve the unpredictable communication needs in wireless communication. The p-persistent CSMA studied in this paper is one of the CSMA with a competitive-based channel access strategy, which provides a flexible frequency resource allocation scheme to maximize the utilization of frequency resources. Meanwhile, by using conflict detection and conflict avoidance mechanisms, random interference in the channel can be effectively handled to improve the reliability and stability of communication, but the performance is better only at low loads. At present, TDMA is more widely used at high load and high speed. Unlike p-persistent CSMA, TDMA divides a channel into a number of independent

Table 1: Table of parameters in the literature.

Literature	Parameter	Meaning
[6]	m	Number of avoidance phases
	N	Number of stations
	τi	Transmission probability of a site in any time slot of the fallback phase i
	P	Probability of conflict
	PE	Probability of channel idleness
[7]	ATIM	Ad hoc traffic indication messages
	Neighbor information list	NIL
	Preferable channel list	PCL
[11]	P_t^S	The transmission power of node S
	P_r^S	The receiving power from node S at node R
	Gt, Gr	Antenna gains of transmitter and receiver
	ht, hr	The heights of the transmit and receive antennas
	d	Distance between transmitter and receiver
	α	Path loss coefficient with range of 2-4
	L	Other losses: assume $L = 1$ here, then c is constant

subchannels according to time, and each subchannel is assigned for the exclusive use of one or more users, which does not have the characteristic of competitive use of channels. TDMA makes full use of the communication channel resources, making it possible to effectively reduce channel conflicts even at high loads, thus improving channel utilization [4, 5]. However, TDMA can hardly cope with the dynamically changing network load, and the TDMA protocol needs to reallocate time slices if new users join or old users drop out during use, which leads to high overhead. In multimedia applications, the TDMA protocol needs to allocate a fixed time slice for each user due to uneven data transmission, and it may not be able to meet the transmission needs of users. In contrast, CSMA performs better in edge server networks with uneven data transmission because the CSMA protocol is more flexible and can dynamically select the appropriate transmission rate according to network demand. Therefore, it becomes especially important to improve the CSMA protocol so that it can provide relatively reliable quality of service even under high load conditions.

2. Related Work

This section highlights current improvements to the CSMA protocol and proposes solutions for improving throughput rates.

In the literature [6], an improved CSMA/CA algorithm for powerline-wireless collaborative communication was proposed for hybrid powerline and wireless networks. The algorithm was compatible with the CSMA/CA algorithm in the existing standards IEEE 1901 and 802.11 and used a two-choice approach for powerline and wireless line idle. The results showed that cooperative communication generally outperforms single-media communication, and throughput performance can be further improved by configuring optimal parameters. However, the system model was based on the decoupling assumption. In practical applications, sites were mostly coupled to each other, so the application of this protocol had some limitations.

The authors in [7] proposed a hybrid protocol H-MMAC protocol based on representatives of three multichannel MAC protocols: dynamic channel assignment (DCA [8]) strategy, multichannel MAC (MMAC [9]), and pipeline multichannel MAC (π-Mc [10]). The hybrid protocol H-MMAC protocol allowed nodes to transmit data packets during the ATIM window, while other nodes tried to negotiate the data channel, which in turn improved the aggregated throughput of the network. However, in the case of multiple channels, if nodes had data to transmit, they must switch the channel from the default channel to the agreed channel and then back to the default channel, which would consume more energy, and the node energy utilization was not high.

In the literature [11], the authors investigated a transmission power control MAC protocol (STPC-MAC) based on the optimization algorithm proposed in [12, 13] for joint rate and power control in wireless networks without interruption constraints. This scheme improved the spatial reuse rate while guaranteeing the SINR at the receiver side. However, due to the need to frequently adjust the transmit power, STPC-MAC introduces time delays, which affected the performance of the system affecting real-time applications. When multiple users perform power adjustment at the same time, it led to system oscillation or instability. In Table 1, we plot the parameters included in the references analyzed above.

The research methods proposed in the above literature for power systems and traditional wireless networks have improved the system throughput rate to some extent, but these improvements are somewhat targeted. They are not

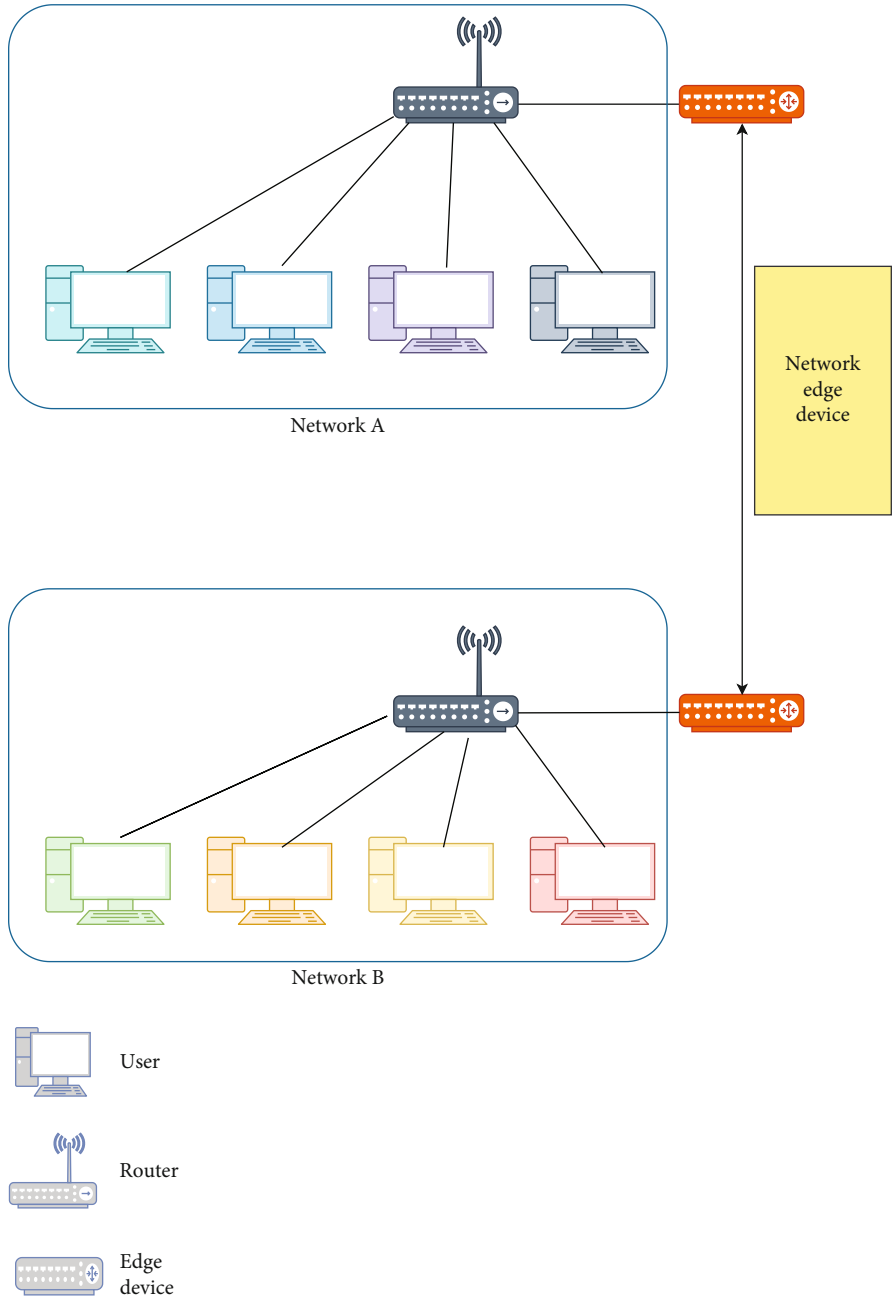

Figure 1: Edge server working diagram.

applicable in edge server networks where the number of access users is relatively large and complex. In order to solve the problem of low throughput rate of the edge server network under high load, we propose a three-time slot P-CSMA protocol with variable success time with multipriority, which solves the problem of low throughput rate of the traditional time-slot CSMA protocol on the one hand; on the other hand, by dividing the multipriority of transmission information, we can provide different number of access edge servers for users with different priorities, thus reducing the information packet transmission failure and improving the throughput rate of the system. The edge service working diagram is shown in Figure 1.

The structure of this paper is as follows: the first part introduces the principle and channel model of the improved protocol and derives the throughput rate, idle rate, and collision rate of the improved protocol, respectively; the second part introduces in detail the principle and channel model of multipriority access to communication channels and then derives the throughput rate of different priorities in the channel; the third part introduces the principle of channel delay and analyzes the average channel delay for single channel and multichannel. In the fourth part, experimental simulations are conducted for the theoretical derivation of the first three parts, and the simulations are analyzed for low and high load volumes. Comparison experiments between

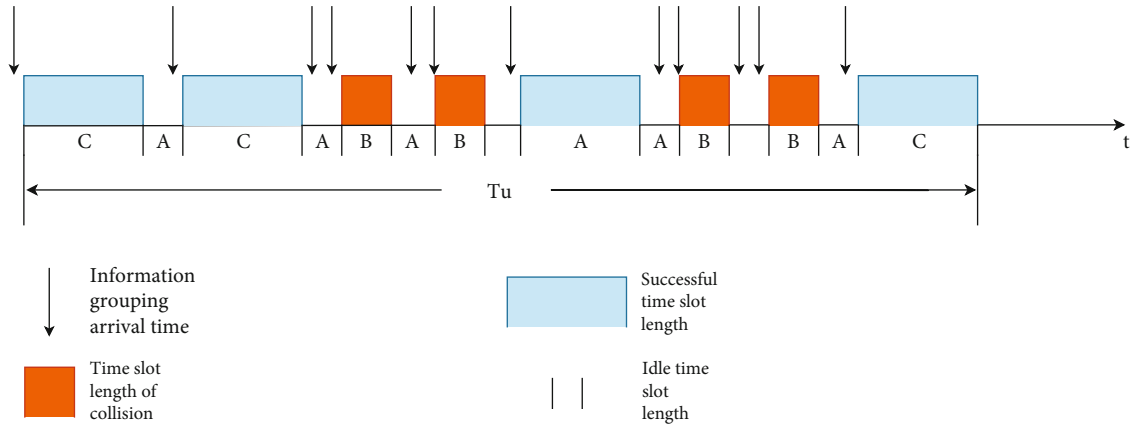

Figure 2: Schematic of the improved protocol.

the new improved protocol and other communication protocols are also included.

Finally, the whole paper is summarized.

3. Analysis of Performance

3.1. Protocol Principle. The three-time slot P-CSMA protocol with variable success length with multiple priorities is based on the traditional nonadherent CSMA protocol. First, the protocol divides the continuous time axis into discrete time slots of different lengths, namely, idle time slot a, collision time slot b, and success time slot c. The width of the time slots is the transmission time of a message packet. All users can access the network channel and start sending data only at the beginning of the time slice synchronously. When a node wants to send data, it first listens to the channel, and if only one information packet arrives in the channel, it sends it successfully; if two or more information packets are connected to the channel at the same time, it decides to continue sending with probability P or abort sending with probability (1-P) and then delays the time slot a and waits for the next time slice to start sending again [14–17].

The model diagram proposed in this paper is shown in Figure 2, and the following assumptions are made for the mathematical model (assuming that the channel is in an ideal operating state with no noise and no interference):

(1) The channel access method is the P-CSMA control protocol; the arrival process of each station on the channel is independent of each other; when the number of stations is large enough, then the distribution on the channel approximates the Poisson distribution (parameter is G)

(2) The state in which the channel is idle is denoted by I, and the length of the idle time slot is a; the state in which the information packet in the channel collides is denoted by B, and the length of the time slot in which the collision occurs is b; the state in which the information packet in the channel is successfully sent is denoted by U, and the length of the successfully sent time slot is c

(3) Listening to the channel first for the duration of idle and collision, and sending messages with probability P when the channel is idle

(4) The number of users on the channel is a Poisson flow

(5) The colliding packets will be retransmitted at a later time, and the retransmitted information packets have no effect on the channel arrival process

3.2. Throughput Analysis. The following assumptions are made about the variables before analyzing the throughput rate (using a single-channel model as an example), and then a table of variables is drawn, as a result of Table 2.

(1) $P\{\mathrm{Nu} = i\}$ denotes the probability distribution function of i consecutive successful events U within a transmission period Tn

(2) $P\{\mathrm{Nbi} = j\}$ denotes the probability distribution function of j consecutive compound events BI in a transmission period Tn;

(3) $P\{\mathrm{Nu} = i, \mathrm{Nbi} = j\}$ denotes the joint probability distribution function of i consecutive successful events U and j compound events BI within a transmission period Tn

(4) Nu denotes the number of i consecutive successful events U in a transmission period Tn;

(5) Nbi denotes the number of j consecutive compound events BI in a transmission period Tn;

(6) Nb denotes the number of collision events in which two and more message packets arrive in a transmission cycle Tn;

(7) Ni denotes the number of idle events I in which no message packet arrives in a transmission cycle Tn,Ni consists of two parts Ni1 and Ni2;

(8) Eu denotes the channel length of a successfully sent message packet in a transmission period Tn;

Table 2: Table of variables.

Symbol	Definition
$P\{\mathrm{Nu} = i\}$	Probability distribution function of i consecutive successful events U in a transmission period Tn
$P\{\mathrm{Nbi} = j\}$	Probability distribution function of$j$consecutive compound events B in a transmission period Tn
$P\{\mathrm{Nu} = i, \mathrm{Nbi} = j\}$	The joint probability distribution function of i consecutive successful events U and j compound events BI in a transmission period Tn
Nu	The number of consecutive i successful events U in a transmission period Tn
Nbi	The number of j consecutive compound events BI in a transmission period Tn
Nb	The number of collision events in which two and more message packets arrive in a transmission period Tn
Ni	The number of idle events I in which no message packet arrives in a transmission cycle Tn
Eu	The length of the channel in which the message packet is successfully sent in a transmission period Tn
Ei	The length of the channel in which no information packet arrives in a transmission period Tn
Eb	The length of the channel in which two and more information packets arrive in the channel in one transmission period Tn
Et	Length of channel time delay
Tn	Channel length for one transmission cycle
Su	Channel throughput rate
Si	Channel idle rate
Sb	Collision rate of the channel
St	Time delay rate of the channel

(9) Ei denotes the length of the channel in which no information packet arrives in a transmission period Tn;

(10) Eb denotes the channel length in which two and more information packets arrive in the channel in one transmission period Tn;

(11) Et denotes the length of the average delay in the channel during a transmission period Tn;

(12) Tn denotes the channel length of a transmission cycle

(13) Su denotes the throughput rate of the channel, Sb denotes the collision rate of the channel, Si denotes the idle rate of the channel, and St denotes the delay rate of the channel

According to the Poisson distribution,

$$P(X = K) = \frac{\lambda^K}{K!} e^{-\lambda}, \tag{1}$$

derives

$$P(X = K) = \frac{(aG)^K}{K!} e^{-aG}, \tag{2}$$

where a is the unit time length, G is the message group arrival rate, and K is the number of arrived message groups.

The probability that only one message packet arrives in time slot c of success period U is given by the following:

$$Pu(1) = cGe^{-cG}. \tag{3}$$

The probability that no message grouping arrives is given by the following:

$$\mathrm{Pu}(0) = e^{-\mathrm{cG}}. \tag{4}$$

The probability that only one message packet arrives in the time slot of the nonsuccessful cycle BI is determined with probability P to be sent by the following:

$$\mathrm{Pbi}(1) = apGe^{-apG}. \tag{5}$$

The probability that no message group arrives is given by:

$$\mathrm{Pbi}(0) = e^{-apG}. \tag{6}$$

According to the derivation, equations (7) and (8) can be obtained

$$P\{\mathrm{Nu} = i\} = \left(cGe^{-cG}\right)^{i-1}\left(1 - cGe^{-cG}\right), \tag{7}$$

$$P\{\mathrm{Nbi} = j\} = \left(1 - apGe^{-apG}\right)^{j-1} apGe^{-apG}. \tag{8}$$

Since the i successful events U and j nonsuccessful events BI occurring consecutively in a transmission

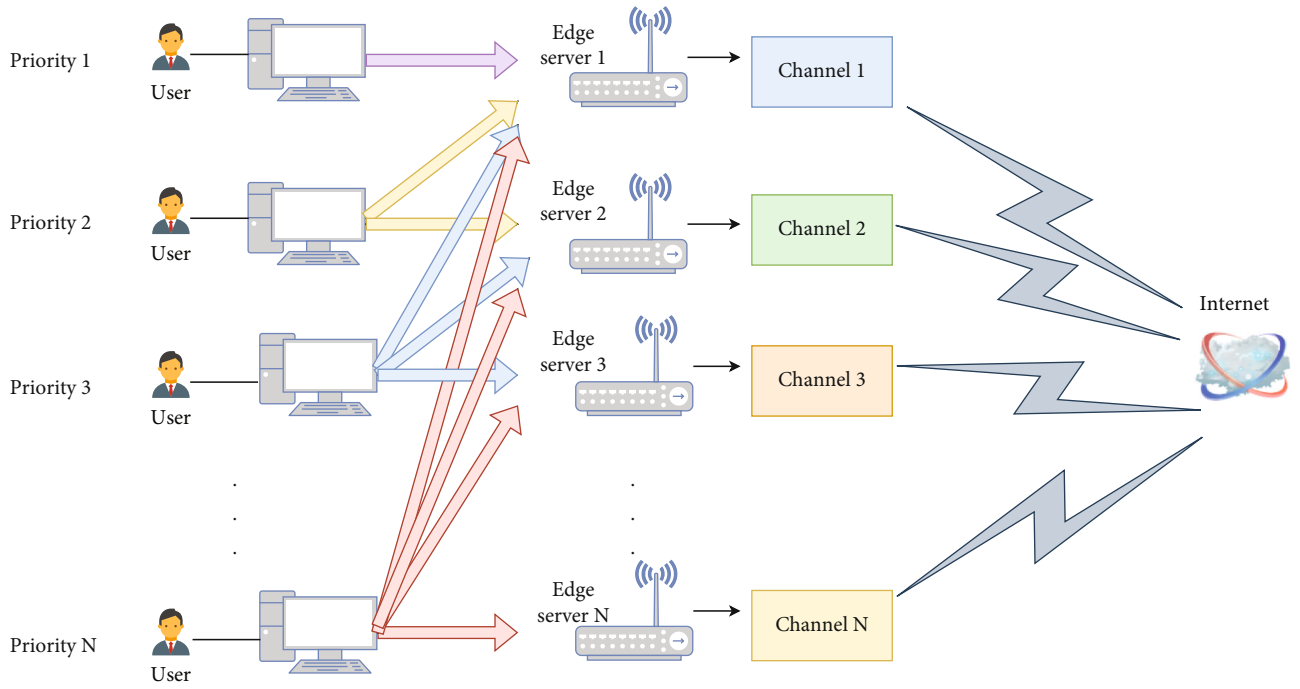

Figure 3: Multipriority access model.

period Tn are independent repeated events, the joint probability distribution is derived from

$$\begin{aligned} P\{\mathrm{Nu}=i,\mathrm{Nbi}=j\} &= P\{\mathrm{Nu}=i\} * P\{\mathrm{Nbi}=j\} \\ &= \left(cGe^{-cG}\right)^{i-1}\left(1-cGe^{-cG}\right) \\ &\quad \cdot \left(1-apGe^{-apG}\right)^{j-1} apGe^{-\mathrm{apG}}. \end{aligned} \tag{9}$$

According to the expectation formula of the joint probability distribution in equation (9) above, the average number of time slots for the successful transmission of message packets U in the channel in a transmission period Tn is obtained from

$$\begin{aligned} Nu &= \sum_{i=1}^{\infty}\sum_{j=1}^{\infty} iP\{Nu=i,Nbi=j\} = \sum_{i=1}^{\infty}\sum_{j=1}^{\infty} i\left(cGe^{-cG}\right)^{i-1} \\ &\quad \cdot \left(1-cGe^{-cG}\right)\left(1-apGe^{-apG}\right)^{j-1} apGe^{-apG} \\ &= \frac{1}{1-cGe^{-cG}}. \end{aligned} \tag{10}$$

Similarly, the average number of time slots of the composite event BI in a transmission period Tn in which no message packet is successfully sent in the channel can be calculated by

$$\begin{aligned} \mathrm{Nbi} &= \sum_{i=1}^{\infty}\sum_{j=1}^{\infty} jP\{\mathrm{Nu}=i,\mathrm{Nbi}=j\} = \sum_{i=1}^{\infty}\sum_{j=1}^{\infty} j\left(cGe^{-cG}\right)^{i-1} \\ &\quad \cdot \left(1-cGe^{-cG}\right)\left(1-apGe^{-apG}\right)^{j-1} apGe^{-apG} \\ &= \frac{1}{apGe^{-apG}}. \end{aligned} \tag{11}$$

The average number of time slots of idle events I in a transmission period Tn in which no information packets arrive in the channel is

$$Ni = Ni1 + Ni2, \tag{12}$$

where Ni1 denotes the number of idle events in the last time slot of successful packets without information packet arrivals and Ni2 denotes the number of idle events in the channel without information packet arrivals in BI consecutive events, so

$$Ni1 = \frac{Pu(0)}{1-Pu(1)} = \frac{e^{-cG}}{1-cGe^{-cG}}, \tag{13}$$

$$Ni2 = Nbi^{*}Pbi(0) = \frac{e^{-apG}}{apGe^{-apG}} = \frac{1}{apG}. \tag{14}$$

From equations (13) and (14), we get Ni

$$\begin{aligned} Ni = Ni1 + Ni2 &= \frac{e^{-cG}}{1-cGe^{-cG}} + \frac{1}{apG} \\ &= \frac{apGe^{-cG}+1-cGe^{-cG}}{apG\left(1-cGe^{-cG}\right)}. \end{aligned} \tag{15}$$

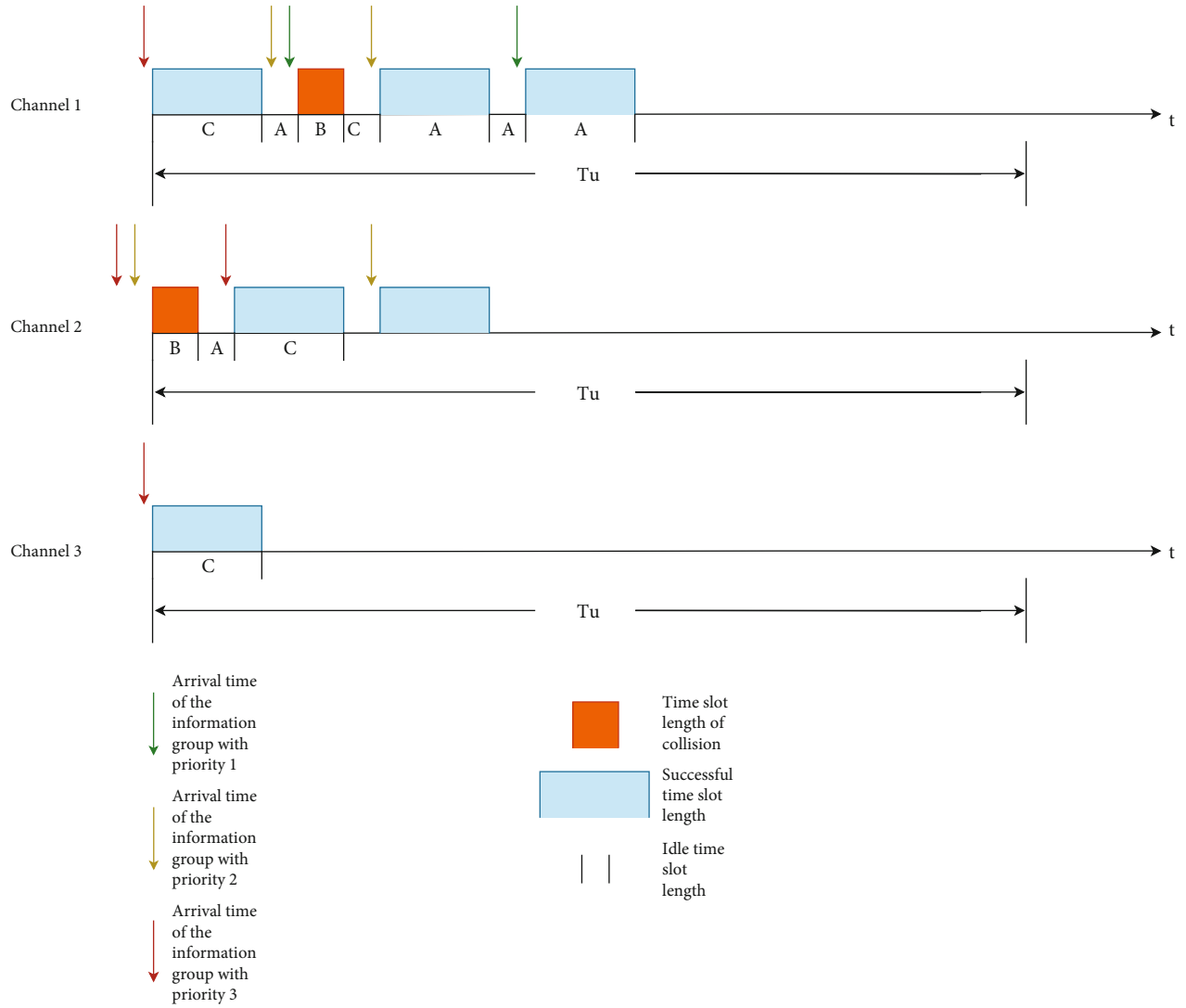

Figure 4: Multipriority timing diagram (with three priority levels as an example).

Since the composite event Nbi is derived from (11), Nb can be derived as

$$Nb = \mathrm{Nbi} - \mathrm{Ni} = \frac{1}{apGe^{-apG}} - \frac{e^{-cG}}{1 - cGe^{-cG}} - \frac{1}{apG} = \frac{1 - cGe^{-cG} - e^{-apG}\left(apGe^{-cG} + 1 - cGe^{-cG}\right)}{apGe^{-apG}\left(1 - cGe^{-cG}\right)}. \tag{16}$$

Therefore, the time slot length Ei of idle events in a transmission cycle is the following:

$$\mathrm{Ei} = \frac{a\left(apGe^{-cG} + 1 - cGe^{-cG}\right)}{apG\left(1 - cGe^{-cG}\right)}. \tag{17}$$

The time slot length Eb of a collision event in one transmission cycle is the following:

$$\mathrm{Eb} = \mathrm{Nb}^* b = \frac{b\left(1 - cGe^{-cG} - e^{-apG}\left(apGe^{-cG} + 1 - cGe^{-cG}\right)\right)}{apGe^{-apG}\left(1 - cGe^{-cG}\right)}. \tag{18}$$

The time slot length of a successful event in a transmission cycle is the following:

$$Eu = Nu^* c = \frac{c}{1 - cGe^{-cG}}. \tag{19}$$

In this paper, assuming that the transmission time

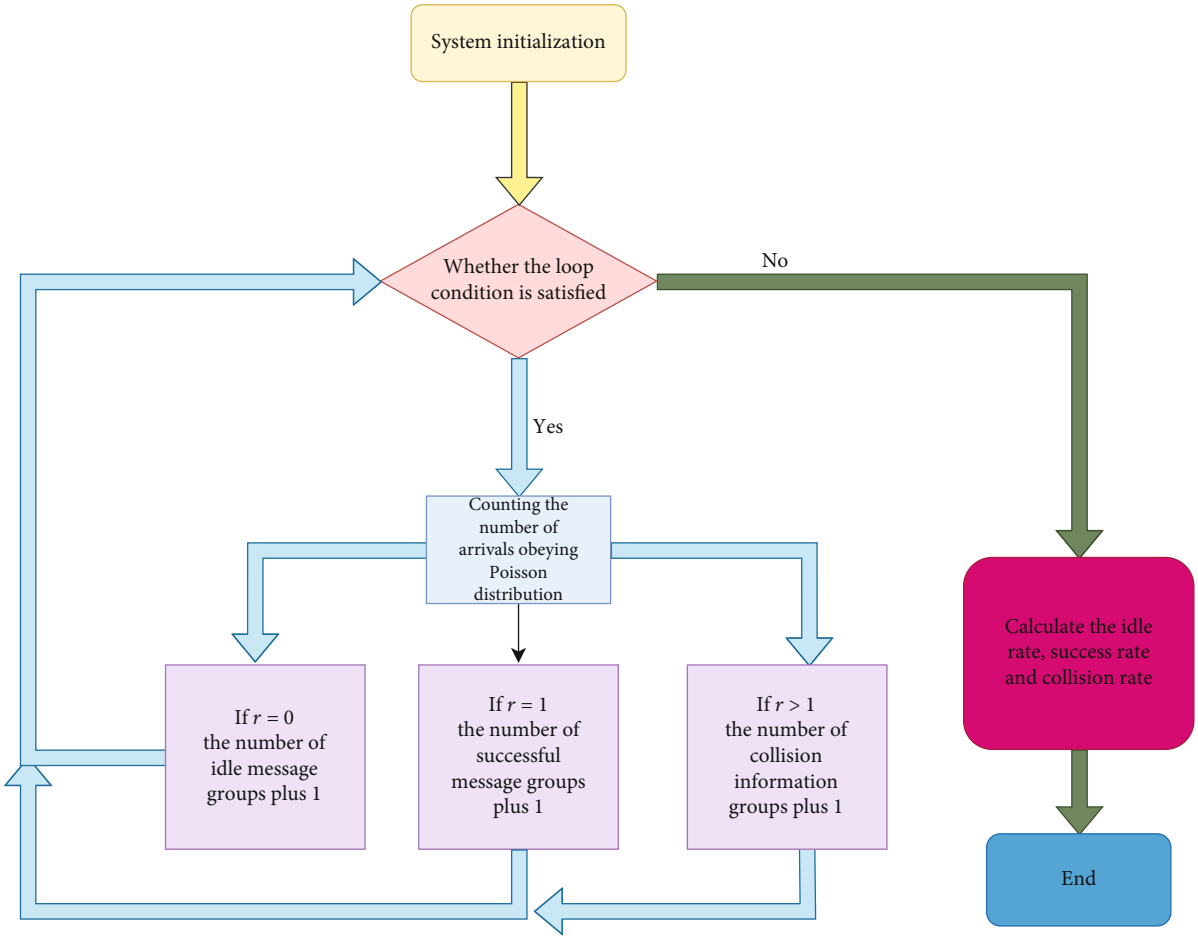

FIGURE 5: Flow chart of simulation experiment.

length and the idle time slot length a are equal, the channel length Tn of one transmission cycle can be obtained as

$$\mathrm{Tn} = \mathrm{Ni} * a + \mathrm{Nb} * (b + a) + \mathrm{Nu} * (c + a), \tag{20}$$

$$\mathrm{Tn} = \mathrm{Ei} + \mathrm{Eu} + \mathrm{Eb} = \frac{ae^{-apG}\left(apGe^{-cG} + 1 - cGe^{-cG}\right) + (b + a)\left(1 - cGe^{-cG} - e^{-apG}\left(apGe^{-cG} + 1 - cGe^{-cG}\right)\right) + a(c + a)pGe^{-apG}}{apGe^{-apG}\left(1 - cGe^{-cG}\right)}. \tag{21}$$

Therefore, based on the throughput rate, equation (22) can be derived

$$\mathrm{Su} = \frac{acpGe^{-apG}}{ae^{-apG}\left(apGe^{-cG} + 1 - cGe^{-cG}\right) + (b + a)\left(1 - cGe^{-cG} - e^{-apG}\left(apGe^{-cG} + 1 - cGe^{-cG}\right)\right) + a(c + a)pGe^{-apG}}. \tag{22}$$

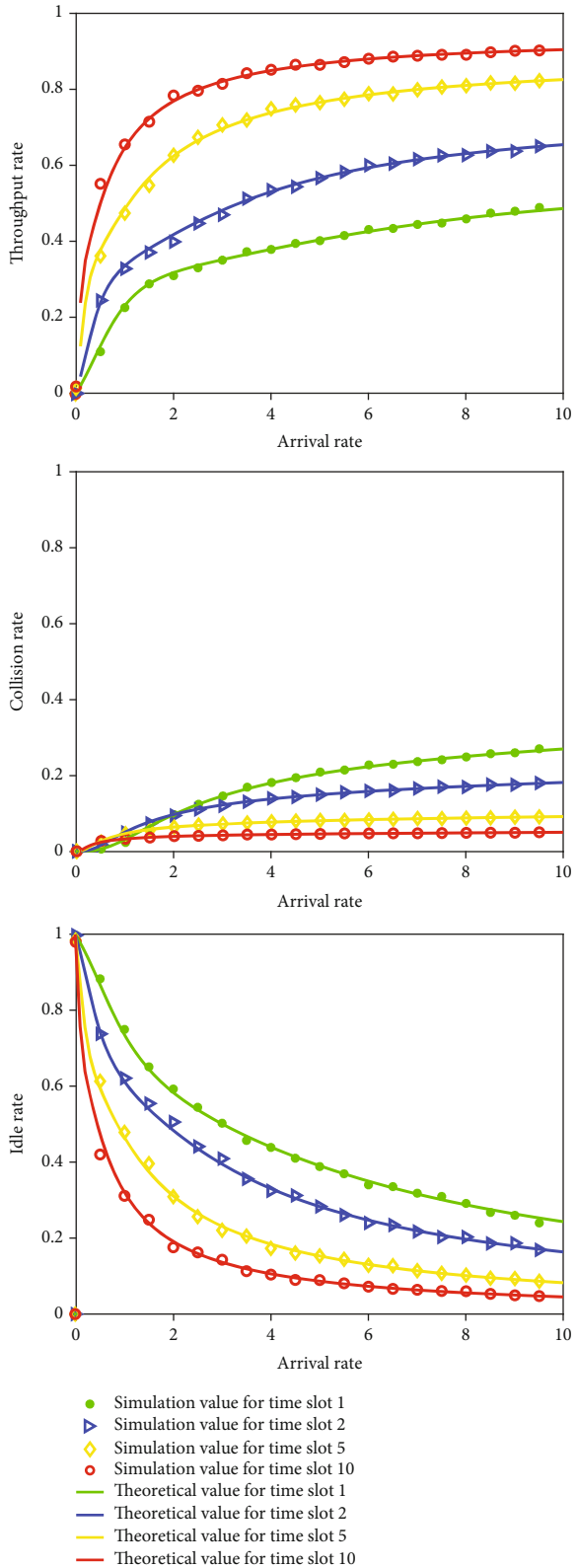

Figure 6: Throughput, collision, and idle rates at low load for $P = 0.2$.

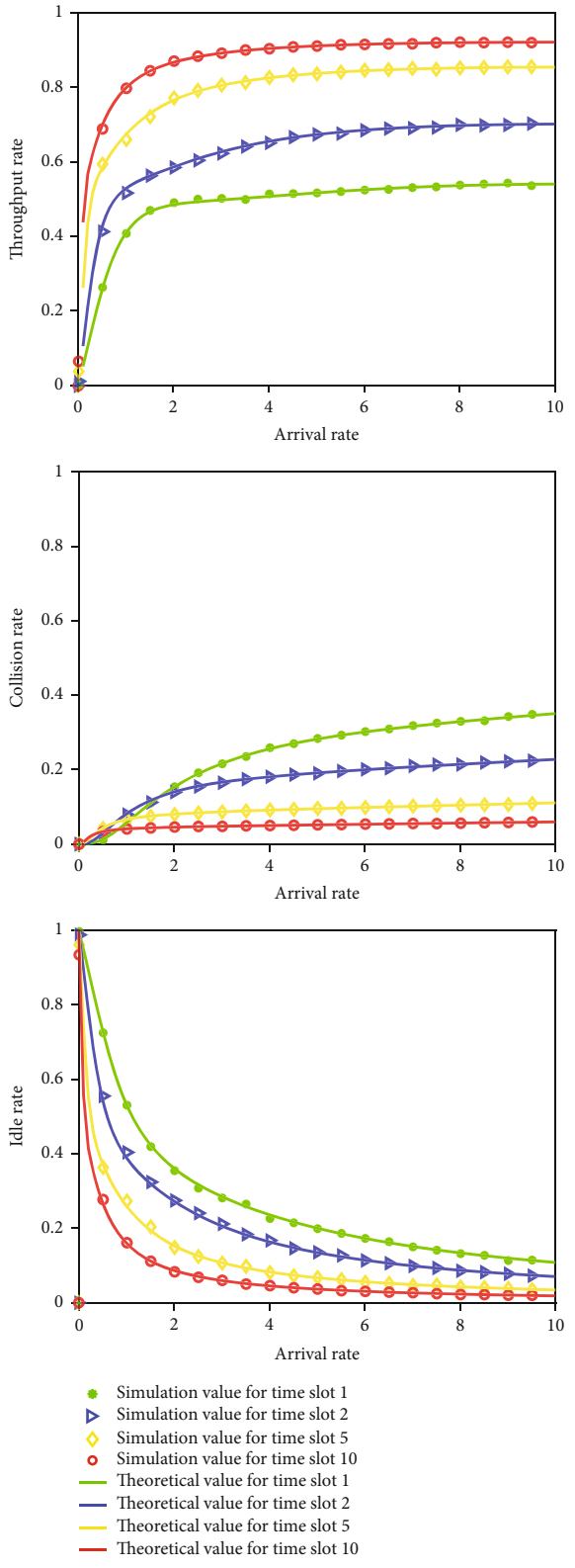

Figure 7: Throughput, collision, and idle rates at low load for $P = 0.5$.

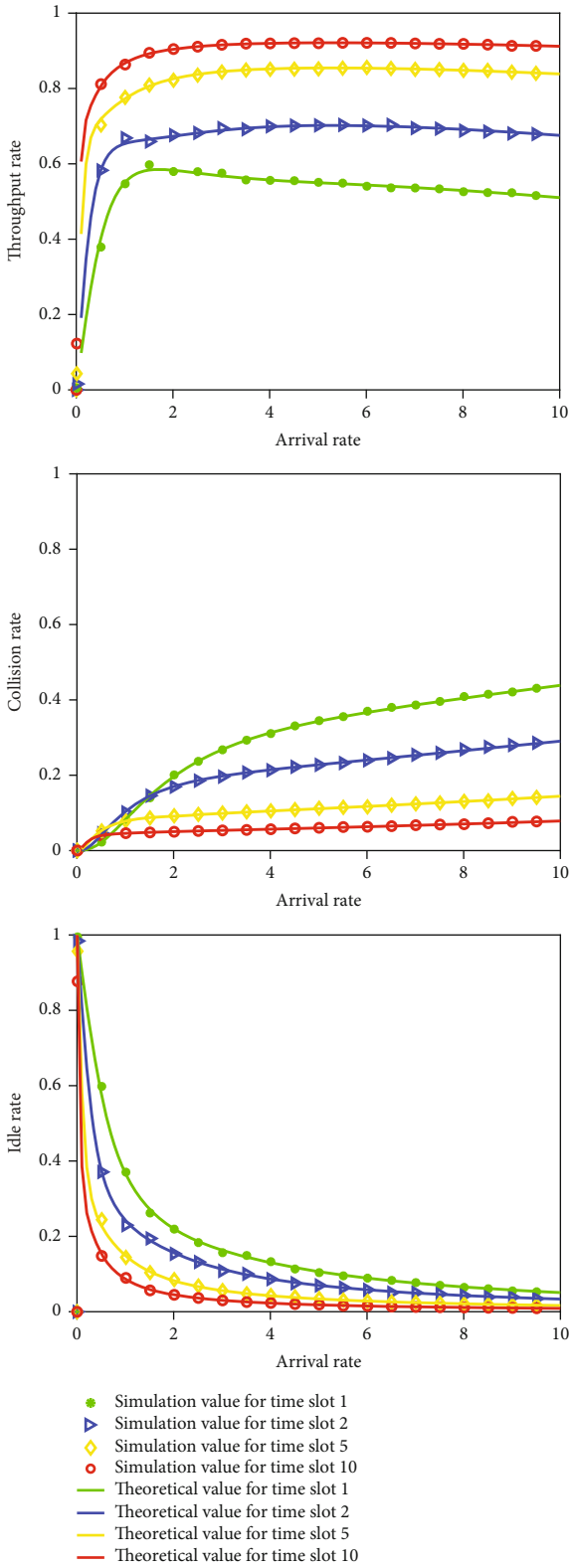

Figure 8: Throughput rate, collision rate, and idle rate at low load for $P = 1$.

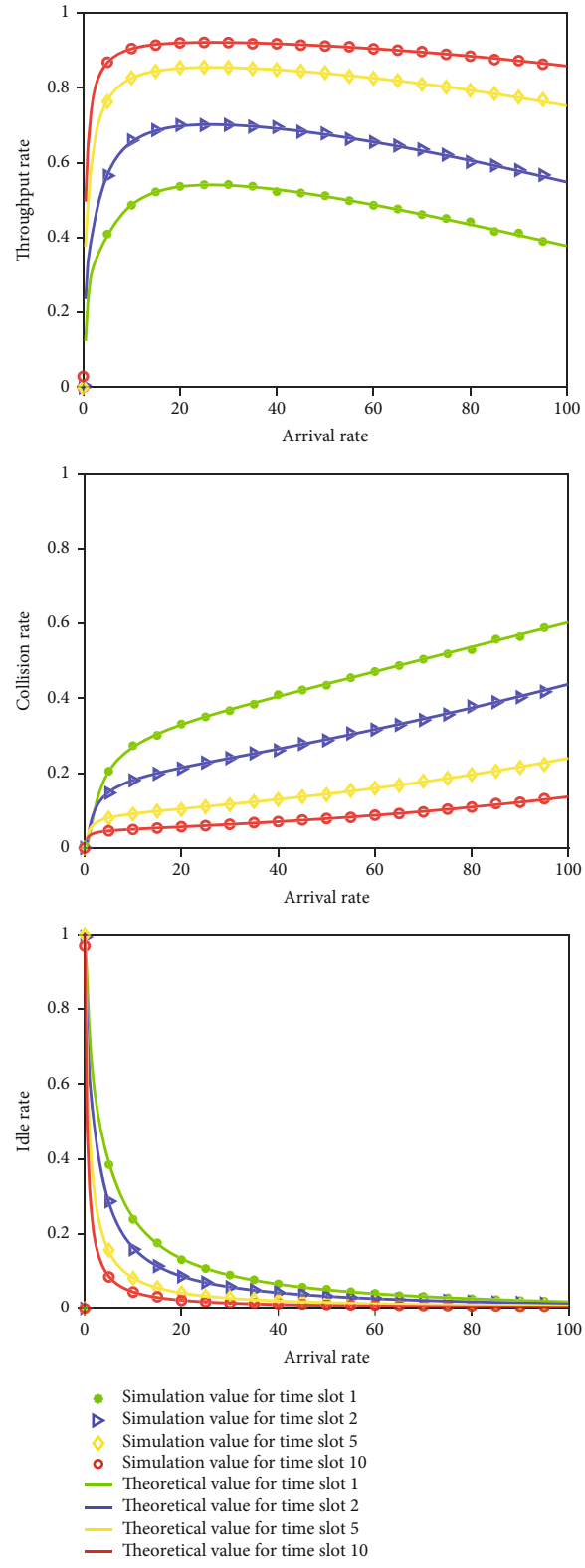

Figure 9: Throughput, collision, and idle rates under high load for $P = 0.2$.

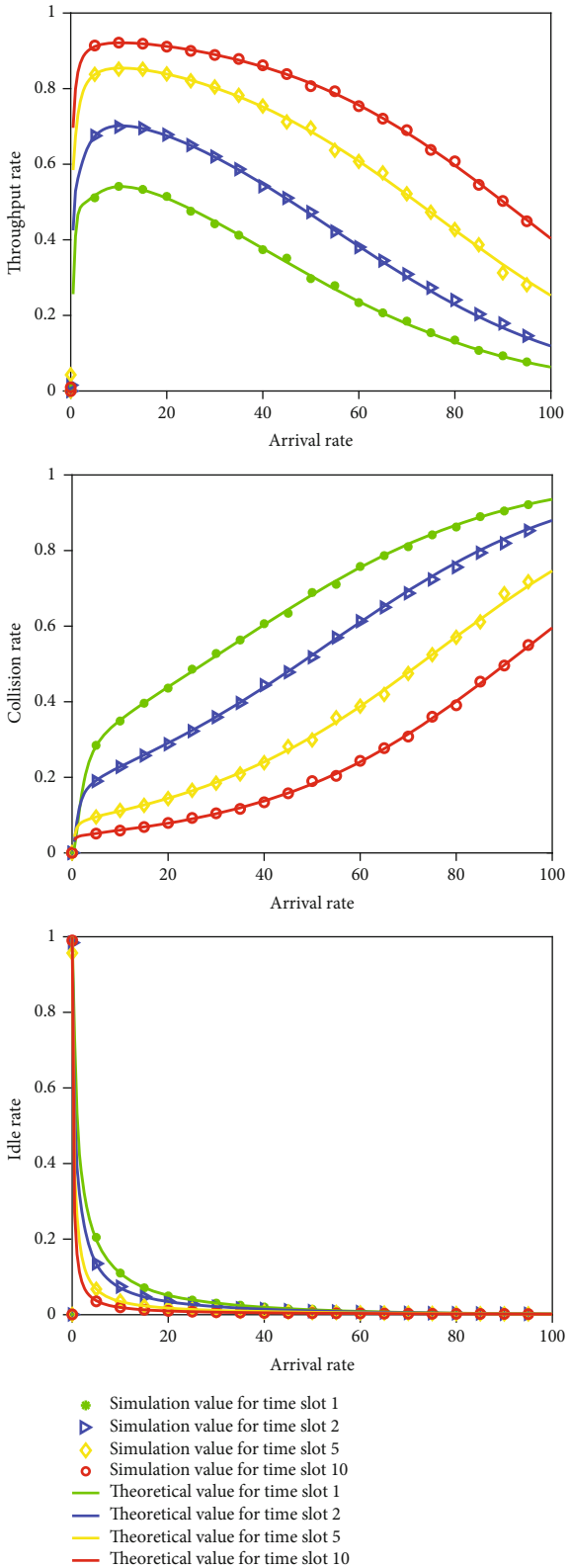

FIGURE 10: Throughput, collision, and idle rates under high load for $P = 0.5$.

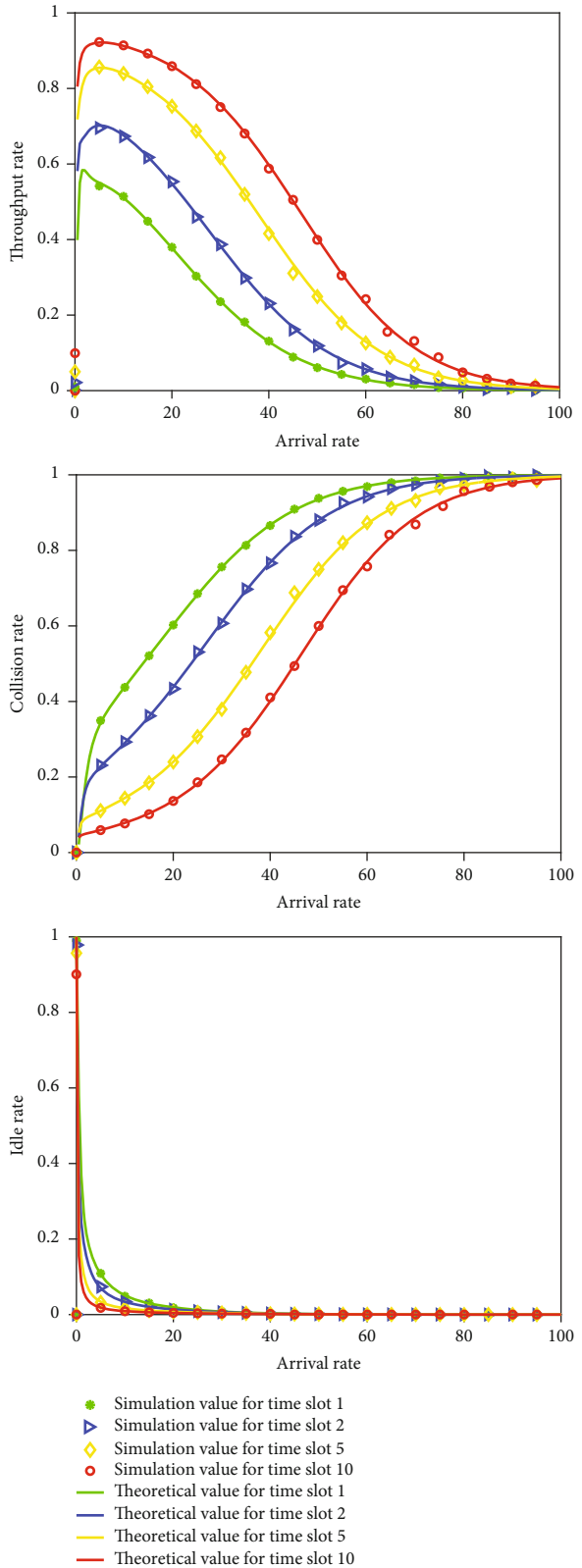

FIGURE 11: Throughput, collision and idle rates under high load for P =1.

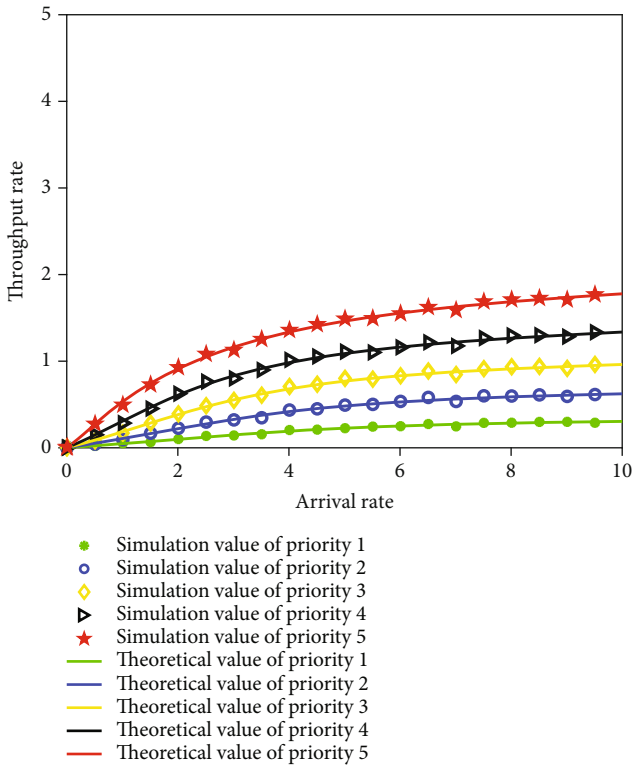

FIGURE 12: $c = 1$, throughput rate for different priority levels under low load.

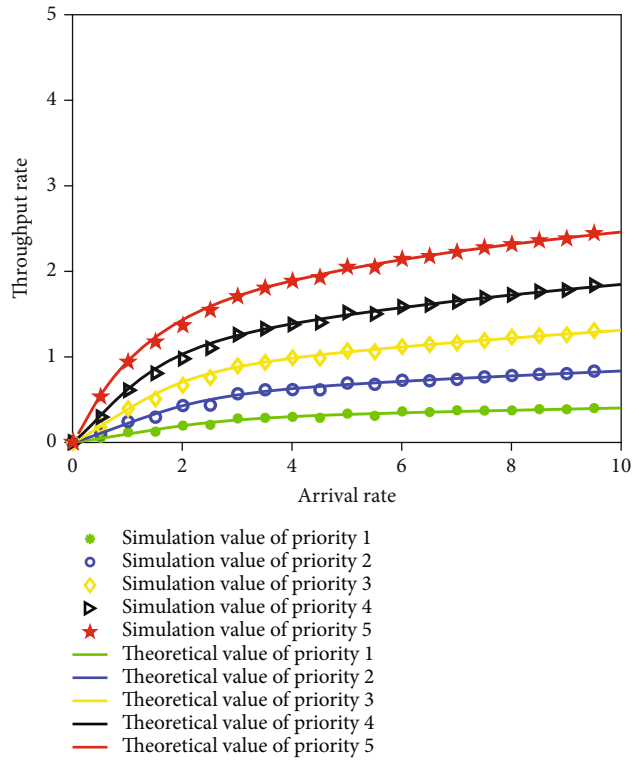

FIGURE 13: $c = 2$, throughput rates for different priority levels under low load.

Similarly, the collision rate of the system can be derived as Eq. (23):

$$\mathrm{Sb} = \frac{\mathrm{Eb}}{\mathrm{Tn}} = \frac{b\left(1 - cGe^{-cG} - e^{-apG}\left(apGe^{-cG} + 1 - cGe^{-cG}\right)\right)}{ae^{-apG}\left(apGe^{-cG} + 1 - cGe^{-cG}\right) + (b+a)\left(1 - cGe^{-cG} - e^{-apG}\left(apGe^{-cG} + 1 - cGe^{-cG}\right)\right) + a(c+a)pGe^{-apG}}. \tag{23}$$

The idle rate of the system is equation (24):

$$Si = \frac{ae^{-apG}\left(apGe^{-cG} + 1 - cGe^{-cG}\right)}{ae^{-apG}\left(apGe^{-cG} + 1 - cGe^{-cG}\right) + (b+a)\left(1 - cGe^{-cG} - e^{-apG}\left(apGe^{-cG} + 1 - cGe^{-cG}\right)\right) + a(c+a)pGe^{-apG}}. \tag{24}$$

4. Multipriority Mechanism for Communication Channels

4.1. Principle of Multipriority Mechanism. Due to the limited channel resources, the probability of simultaneous message access to the channel increases when the number of message packet arrival rates is too large. Too many random accesses cause a sharp decrease in the throughput rate of the communication system and a subsequent increase in the collision rate, which leads to a waste of channel resources and energy. In order to reduce the collision of message packets and improve the throughput rate of the communication system when the amount of information is too large, a multipriority mechanism is incorporated [18–20]. The information packets sent by users are classified into different priorities according to their different service requirements, and the number of edge servers occupied by different priorities when accessing the channel is different. Assume that the communication system consists of N channels and that there are N message packet priorities. The information packets are sorted according to priority, from 1 to N. The information packet with priority 1 can occupy channel 1 for sending, the packet with priority 2 can occupy two channels, i.e., channels 1 and 2 for sending, and so on, and the packet with

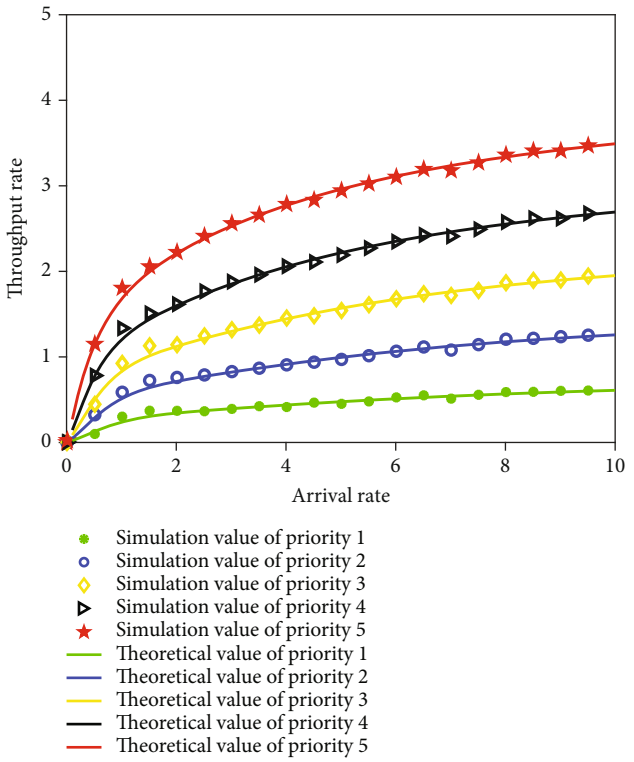

FIGURE 14: $c = 5$, throughput rates for different priority levels under low load.

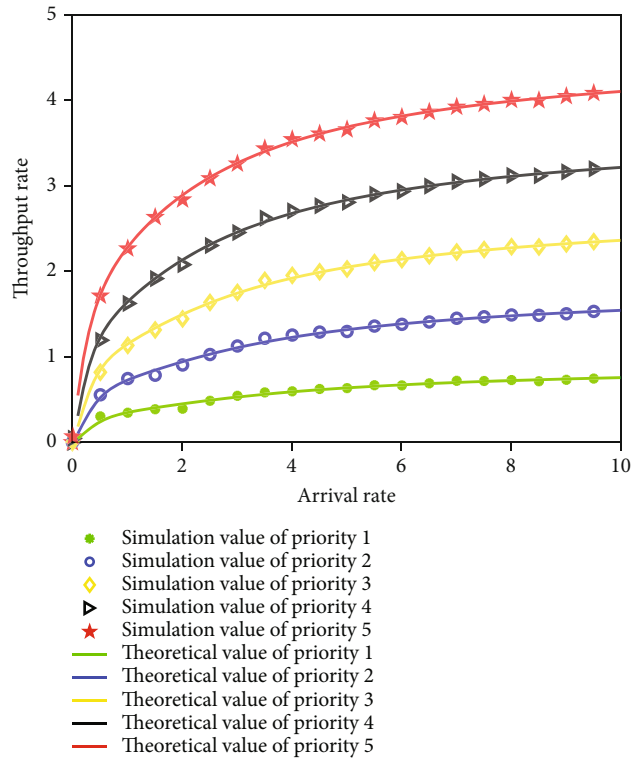

FIGURE 15: $c = 10$, throughput rates for different priority levels under low load.

priority N can occupy channels 1 to N. In the deployment of edge servers, the higher the priority, the more users can occupy the number of servers [17]. The multipriority access model is shown in Figure 3, and the timing diagram is shown in Figure 4.

4.2. Multipriority Theory Derivation. Based on the principle of the multipriority mechanism, the throughput rate of a message grouping with priority 1 can be derived, as shown in

$$\mathrm{Su1} = \frac{acp(G/N)e^{-ap(G/N)}}{ae^{-ap(G/N)}\left(ap(G/N)e^{-c(G/N)} + 1 - c(G/N)e^{-c(G/N)}\right) + (b+a)\left(1 - c(G/N)e^{-c(G/N)} - e^{-ap(G/N)}\left(ap(G/N)e^{-c(G/N)} + 1 - c(G/N)e^{-c(G/N)}\right)\right) + a(c+a)p(G/N)e^{-ap(G/N)}}. \tag{25}$$

Similarly, the throughput rate of a message grouping with priority 2 is shown in

$$\mathrm{Su21} = \frac{acp(G/N)e^{-ap(G/N)}}{ae^{-ap(G/N)}\left(ap(G/N)e^{-c(G/N)} + 1 - c(G/N)e^{-c(G/N)}\right) + (b+a)\left(1 - c(G/N)e^{-c(G/N)} - e^{-ap(G/N)}\left(ap(G/N)e^{-c(G/N)} + 1 - c(G/N)e^{-c(G/N)}\right)\right) + a(c+a)p(G/N)e^{-ap(G/N)}}, \tag{26}$$

$$\mathrm{Su22} = \frac{acp(G/(N-1))e^{-ap(G/N-1)}}{ae^{-ap(G/N-1)}\left(ap(G/(N-1))e^{-c(G/(N-1))} + 1 - c(G/(N-1))e^{-c(G/N-1)}\right) + (b+a)\left(1 - c(G/(N-1))e^{-c(G/N-1)} - e^{-ap(G/N-1)}\left(ap(G/(N-1))e^{-c(G/(N-1))} + 1 - c(G/(N-1))e^{-c(G/N-1)}\right)\right) + a(c+a)p(G/(N-1))e^{-ap(G/N-1)}}, \tag{27}$$

$$\mathrm{Su2} = \mathrm{Su21} + \mathrm{Su22} = \sum_{x=1}^{2}\left(\frac{acp(G/N-x+1)e^{-ap(G/(N-x+1))}}{ae^{-ap(G/(N-x+1))}\left(ap(G/(N-x+1))e^{-c(G/(N-x+1))} + 1 - c(G/(N-x+1))e^{-c(G/(N-x+1))}\right) + (b+a)\left(1 - c(G/(N-x+1))e^{-c(G/N-x+1)} - e^{-ap(G/(N-x+1))}\left(ap(G/(N-x+1))e^{-c(G/(N-x+1))} + 1 - c(G/(N-x+1))e^{-c(G/(N-x+1))}\right)\right) + a(c+a)p(G/(N-x+1))e^{-ap(G/(N-x+1))}}\right). \tag{28}$$

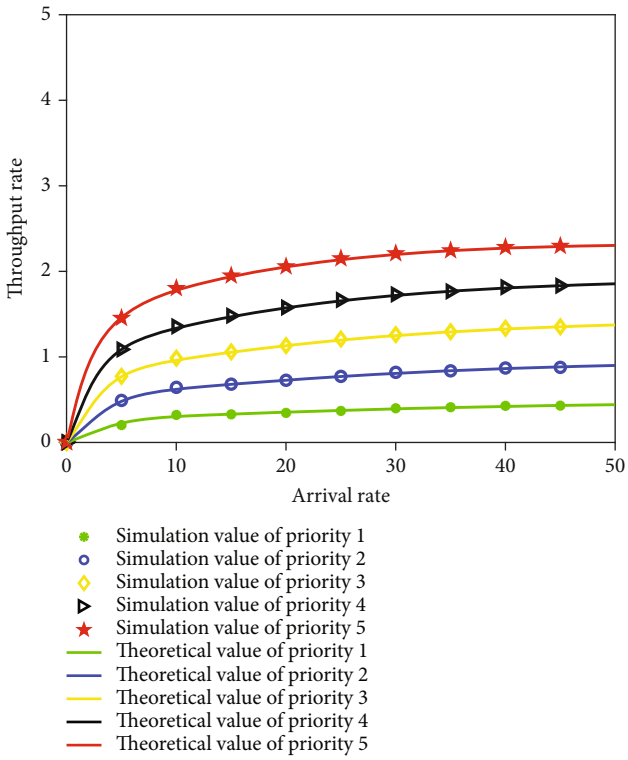

FIGURE 16: $C = 1$ Throughput rate for different priority levels under high load.

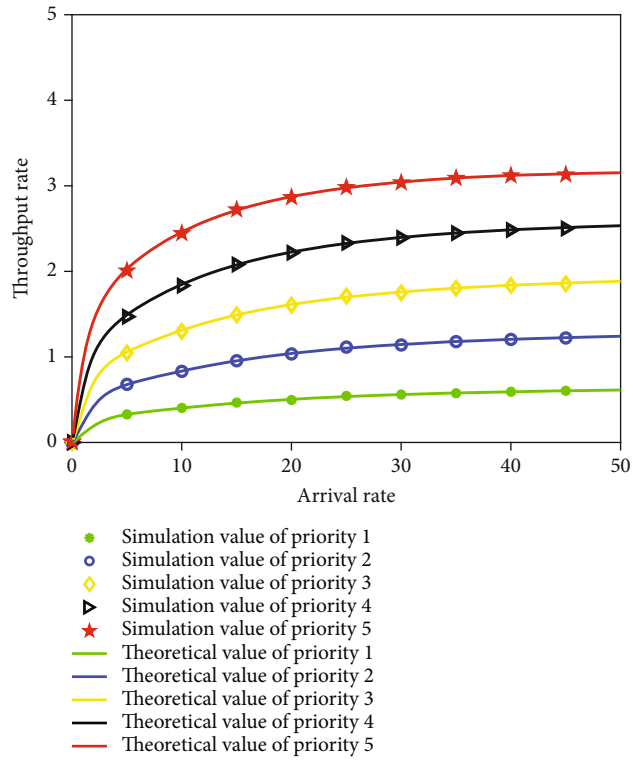

FIGURE 17: $C = 2$ Throughput rate for different priority levels under high load.

Therefore, the throughput rate of a message grouping with priority r is shown in

$$\begin{aligned}\mathrm{Sur} &= \sum_{x=1}^{r}\left(\frac{acp(G/(N-x+1))e^{-ap(G/(N-x+1))}}{ae^{-ap(G/(N-x+1))}\left(ap(G/(N-x+1))e^{-c(G/(N-x+1))}+1-c(G/(N-x+1))e^{-c(G/(N-x+1))}\right)+(b+a)\left(1-c(G/(N-x+1))e^{-c(G/(N-x+1))}-e^{-ap(G/(N-x+1))}\left(ap(G/(N-x+1))e^{-c(G/(N-x+1))}+1-c(G/N-x+1)e^{-c(G/(N-x+1))}\right)\right)+a(c+a)p(G/(N-x+1))e^{-ap(G/(N-x+1))}}\right)\\ &= \sum_{x=1}^{r}\left((G/(N-x+1))\right)\frac{acpGe^{-apG}}{ae^{-apG}\left(apGe^{-cG}+1-cGe^{-cG}\right)+(b+a)\left(1-cGe^{-cG}-e^{-apG}\left(apGe^{-cG}+1-cGe^{-cG}\right)\right)+a(c+a)pGe^{-apG}}.\end{aligned} \tag{29}$$

5. System Average Delay Derivation

5.1. Average Delay of Single Channel System. According to the principle of the protocol proposed in this paper, the propagation delay of each information packet in a busy cycle is a, and it is assumed that the idle time slot is not a delay time slot. The average delay is the ratio of the total delay of collision and successful message packets in one transmission cycle to the length of one transmission cycle.

According to the above equations (10) and (16), it is obtained that

$$\begin{aligned}\mathrm{Et} &= a^{*}(\mathrm{Nu}+\mathrm{Nb}),\\ Et &= a^{*}\left(\frac{1}{1-cGe^{-cG}}+\frac{1-cGe^{-cG}-e^{-apG}\left(apGe^{-cG}+1-cGe^{-cG}\right)}{apGe^{-apG}\left(1-cGe^{-cG}\right)}\right).\end{aligned} \tag{30}$$

Therefore, the average time delay St is

$$St = \frac{Et}{Tn}$$

$$\begin{aligned}\mathrm{St} &= \frac{a^{*}\left(\left(1/1-cGe^{-cG}\right)+\left(\left(1-cGe^{-cG}-e^{-apG}\left(apGe^{-cG}+1-cGe^{-cG}\right)\right)/apGe^{-apG}\left(1-cGe^{-cG}\right)\right)\right)}{\left(\left(ae^{-apG}\left(apGe^{-cG}+1-cGe^{-cG}\right)+(b+a)\left(1-cGe^{-cG}-e^{-apG}\left(apGe^{-cG}+1-cGe^{-cG}\right)\right)+a(c+a)pGe^{-apG}\right)/apGe^{-apG}\left(1-cGe^{-cG}\right)\right)}\\ &= \frac{a^{*}\left(\left(1/\left(1-cGe^{-cG}\right)\right)+\left(\left(1-cGe^{-cG}-e^{-apG}\left(apGe^{-cG}+1-cGe^{-cG}\right)\right)/apGe^{-apG}\left(1-cGe^{-cG}\right)\right)\right)*apGe^{-apG}\left(1-cGe^{-cG}\right)}{ae^{-apG}\left(apGe^{-cG}+1-cGe^{-cG}\right)+(b+a)\left(1-cGe^{-cG}-e^{-apG}\left(apGe^{-cG}+1-cGe^{-cG}\right)\right)+a(c+a)pGe^{-apG}}.\end{aligned} \tag{31}$$

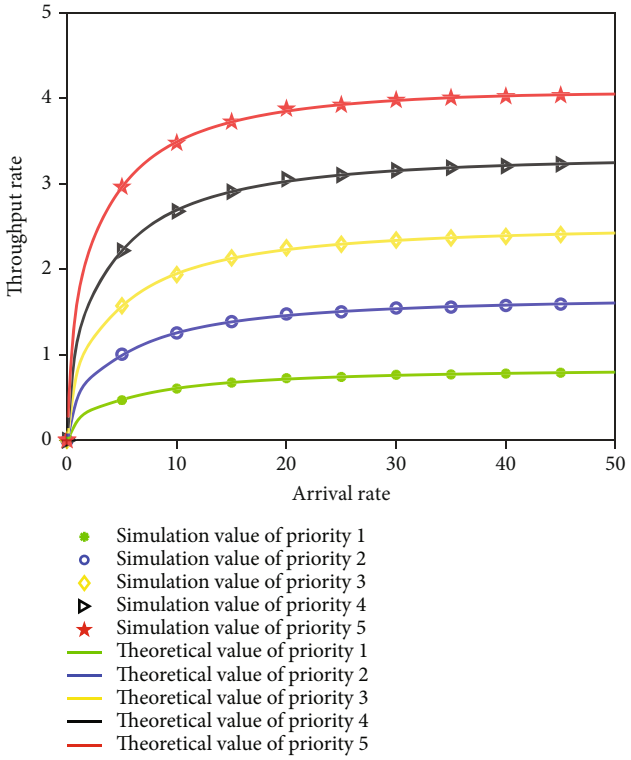

FIGURE 18: $C = 5$ Throughput rate for different priority levels under high load.

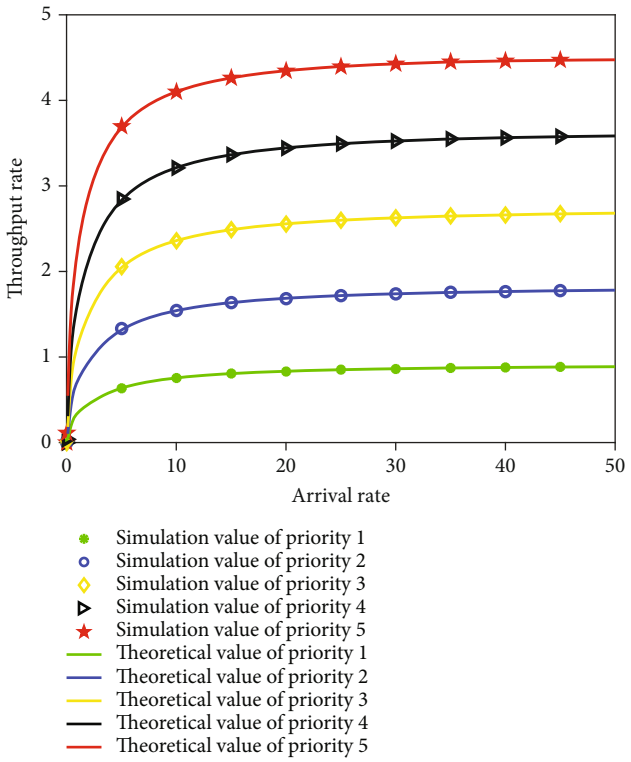

FIGURE 19: $C = 10$ Throughput rate for different priority levels under high load.

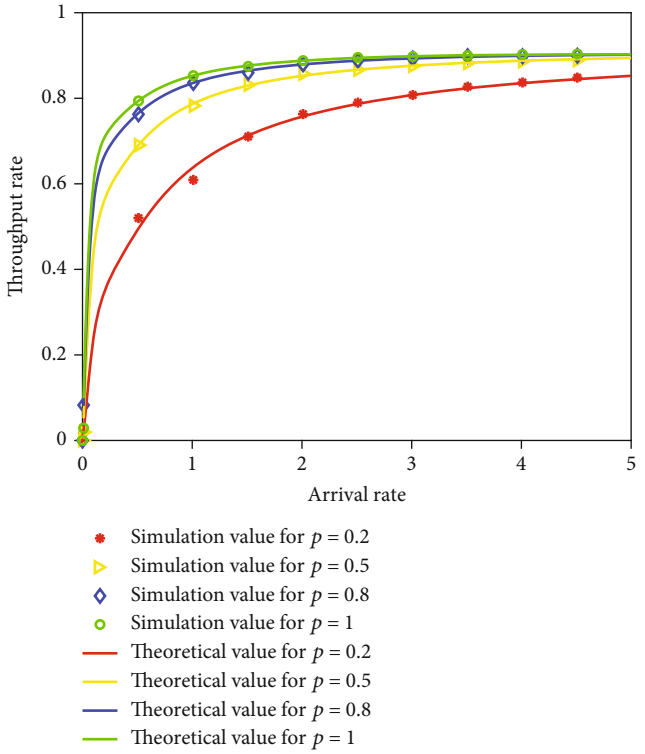

FIGURE 20: Throughput of the system for different values of P.

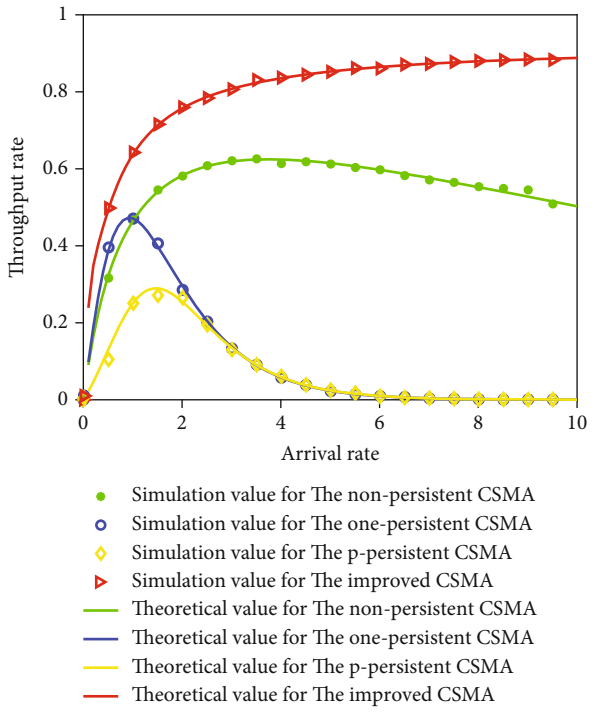

FIGURE 21: System throughput for different protocols.

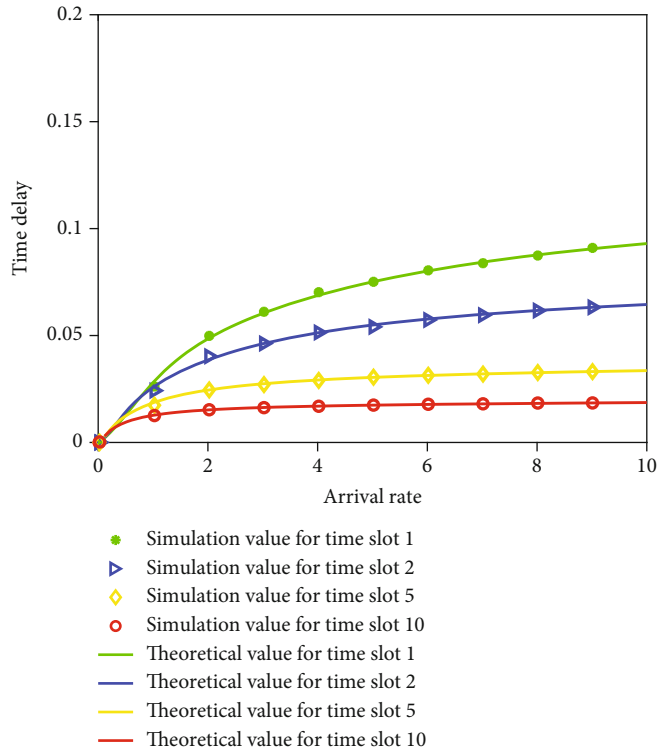

Figure 22: Average delay of a single channel under low load.

5.2. Average Delay for Multichannel Multipriority Systems. Based on the theoretical derivation of multipriority, it is known that the message grouping delay with priority 1 is

$$\mathrm{St1} = \frac{a^*\left(1 - c(G/N)e^{-c(G/N)} - e^{-ap(G/N)}\left(ap(G/N)e^{-c(G/N)} + 1 - c(G/N)e^{-c(G/N)}\right)\right) * ap(G/N)e^{-ap(G/N)}\left(1 - c(G/N)e^{-c(G/N)}\right)}{ae^{-ap(G/N)}\left(ap(G/N)e^{-c(G/N)} + 1 - c(G/N)e^{-c(G/N)}\right) + (b+a)\left(1 - c(G/N)e^{-c(G/N)} - e^{-ap(G/N)}\left(ap(G/N)e^{-c(G/N)} + 1 - c(G/N)e^{-c(G/N)}\right)\right) + a(c+a)p(G/N)e^{-ap(G/N)}}. \tag{32}$$

The delay of a message packet with priority 2 is

$$\mathrm{St2} = \sum_{x=1}^{2} \frac{a^*\left(\left(1/1 - c(G/(N-x+1))e^{-c(G/(N-x+1))}\right)\right) + \left(1 - c(G/(N-x+1))e^{-c(G/(N-x+1))} - e - e^{-ap(G/(N-x+1))}\left(\mathrm{ap}(G/(N-x+1))e^{-c(G/(N-x+1))} + 1 - c(G/(N-x+1))e^{-c(G/(N-x+1))}\right)/\mathrm{ap}(G/(N-x+1))e^{\mathrm{ap}(G/(N-x+1))}\left(1 - c(G/(N-x+1))e^{-c(G/(N-x+1))}\right)\right) * \mathrm{ap}(G/(N-x+1))e^{\mathrm{ap}(G/(N-x+1))}\left(1 - c(G/N-x+1)\right)e^{-c(G/(N-x+1))}}{\mathrm{ae}^{-\mathrm{ap}(G/(N-x+1))}\left(\mathrm{ap}(G/(N-x+1))e^{-c(G/(N-x+1))} + 1 - c(G/(N-x+1))e^{-c(G/(N-x+1))}\right) + (b+a)\left(1 - c(G/(N-x+1))e^{-c(G/(N-x+1))} - e^{-ap(G/(N-x+1))}\left(\mathrm{ap}(G/(N-x+1))e^{-c(G/(N-x+1))} + 1 - c(G/(N-x+1))e^{N-x+1}\right)\right) + a(c+a)p(G/(N-x+1))e^{-ap(G/(N-x+1))}}. \tag{33}$$

The time delay of a message packet with priority r is

$$\mathrm{Str} = \sum_{x=1}^{r}\left(1/(N-x+1)\right)\frac{a^*\left(\left(1/\left(1 - cGe^{-cG}\right)\right) + \left(1 - cGe^{-cG} - e^{-apG}\left(\mathrm{ap}Ge^{-cG} + 1 - cGe^{-cG}\right)/apGe^{-apG}\left(1 - cGe^{-cG}\right)\right)\right) * apGe^{-apG}\left(1 - cGe^{-cG}\right)}{ae^{-apG}\left(apGe^{-cG} + 1 - cGe^{-cG}\right) + (b+a)\left(1 - cGe^{-cG} - e^{-apG}\left(apGe^{-cG} + 1 - cGe^{-cG}\right)\right) + a(c+a)pGe^{-apG}}. \tag{34}$$

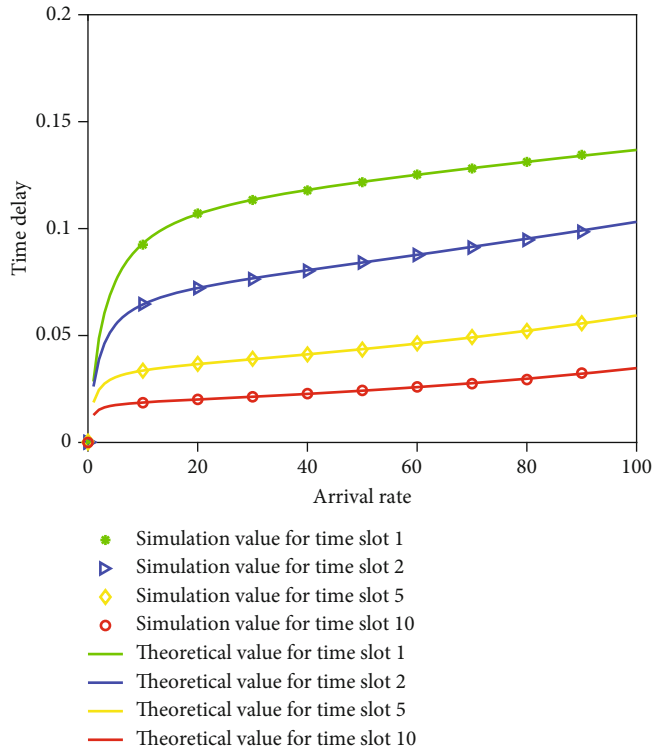

Figure 23: Average delay of a single channel under high load.

6. Analysis of Simulation Experiments

6.1. Flow of Simulation Experiment Procedure. This experimental simulation program is designed and implemented by MATLAB R2018b software. The number of information grouping arrivals in the program relies on the Poisson distribution function for random generation, and the program flowchart is shown in Figure 5.

In this MATLAB simulation, the Poisson distribution function is used to generate the number of random events, and the number is considered the number of simultaneous arrivals of information groups. In order to avoid the chance of the experiment and increase the credibility of the experimental data, the function is embedded in *a* for loop, which generates 10,000 random numbers satisfying the distribution. The loop condition in the above figure is whether 10,000 random numbers are generated using the Poisson distribution function, and the loop is jumped out when the condition is satisfied. Finally, we will count the number of collisions, idle, and successful message groupings, respectively.

6.2. Experimental Analysis of Throughput Rate, Collision Rate, and Idle Rate of the System under Single Channel

6.2.1. Experimental Results in a Low Competition Scenario (with the Highest Arrival Rate of 10 to Simulate a Low Competition Scenario). The idle time slot length a is taken as 0.1, and the collision time slot length b is taken as 0.5 in the simulation experiment.

According to Figures 6–8, the throughput rate of the system increases gradually, the collision rate increases, and the idle rate decreases gradually from 1 to 0. The difference is that the larger the success time slot value, the larger the throughput rate of the system when the arrival rate is the same. Regardless of the value of P and the size of c, the system metrics reach the inflection point when the arrival rate is close to 2. The maximum throughput rate of the system is close to 0.9, and the maximum collision rate is less than 0.1 when $c = 10$, and close to 0.5 and 0.25 when $c = 1$. It can also be seen that the larger the value of P, the faster the throughput rate reaches a relatively stable state when the arrival rate is small. For example, with $P = 1$, the throughput rate reaches its maximum when the arrival rate is about 2 and the collision rate starts to rise sharply; with $P = 0.2$, the throughput rate of the system reaches its maximum when the arrival rate reaches about 10. The different values of P have less impact on the maximum value of the throughput rate, and with three probability values, the maximum throughput rate is about 0.5 with $c = 1$, about 0.65 with $c = 2$, and about 0.82 with $c = 5$ The maximum throughput rate is about 0.82, and the maximum throughput rate for $c = 10$ is about 0.9. Thus, it can be seen that the size of the success time slot affects the maximum throughput rate of the system, and the size of the P value affects the size of the arrival rate corresponding to the maximum throughput rate when the system is taken.

Figure 6 shows the curves of throughput, collision rate, and idle rate of the channel with arrival rate G for successful time slots of 1, 2, 5, and 10 time slot lengths at low load with transmission probability $P = 0.2$. Regardless of the value of c, the throughput rate and collision rate increase gradually with increasing arrival rate, and the idle rate decreases

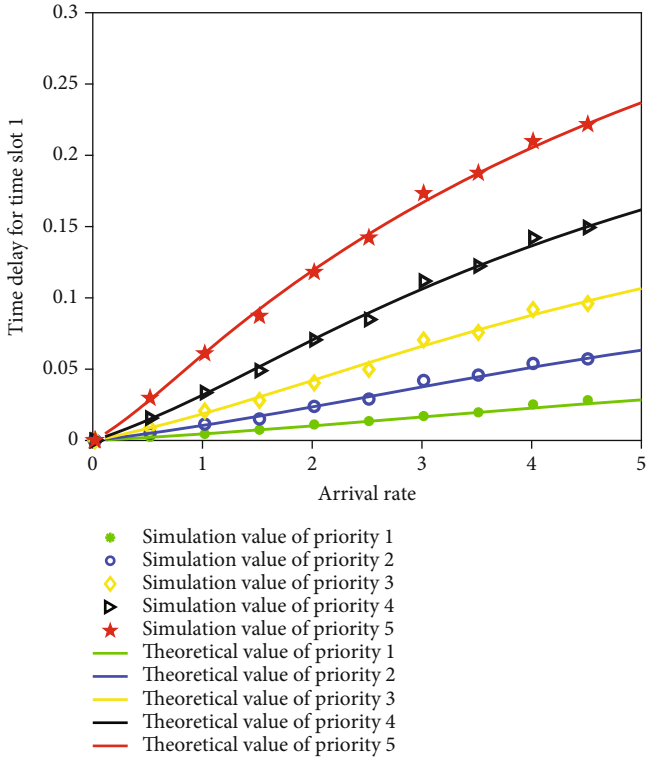

Figure 24: Average delay for $c = 1$ low load multipriority.

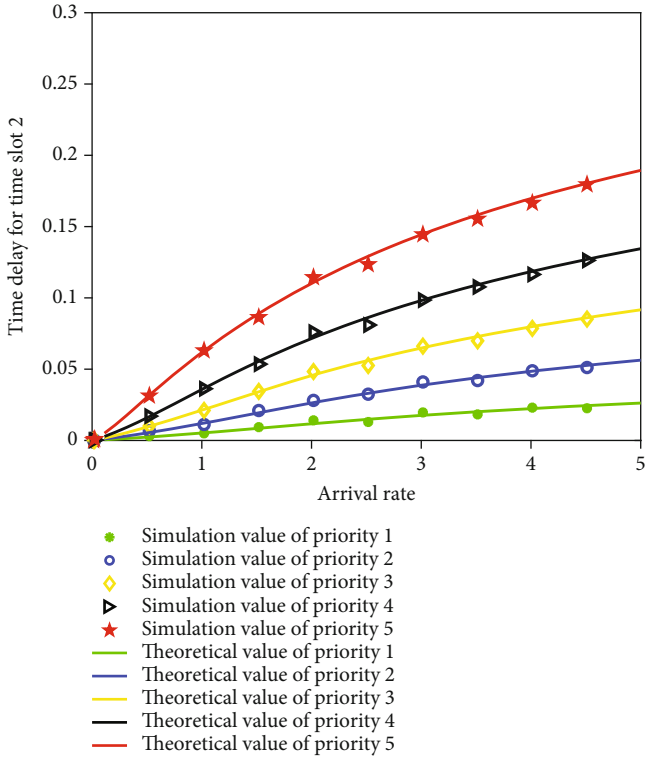

Figure 25: Average delay for $c = 2$ low load multipriority.

gradually to 0 with increasing arrival rate. $c = 1$, the corresponding maximum throughput rate is close to 0.5; $c = 2$, the corresponding maximum throughput rate is close to 0.65; $c = 5$, the corresponding maximum throughput rate is close to 0.82; $c = 10$, the corresponding maximum throughput rate is close to 0.9. The throughput rate of the channel corresponding to $c = 10$ is consistently higher than that of the case when c is taken as 1, 2, and 5, regardless of the size of G. It can also be seen that the collision and idle rates of the system are smaller for the same value of c than for the case when the load G is taken as 1, 2, and 5 timeslots. It shows that the longer success time slot is equivalent to reducing the length of the time slot occupied by the collision and idle message groups, so the collision and idle rates of the system will decrease and the throughput rate will increase, while the collision time slot length remains unchanged.

Figure 7 shows the throughput, collision, and idle rates of the channel with arrival rate G for successful time slots of 1, 2, 5, and 10 time slot lengths at low load with transmission probability $P = 0.5$. Unlike the case of $P = 0.2$, the throughput rate of the system basically does not change for arrival rates greater than 2, regardless of the value of c. The similarity is that the higher the value of c, the higher the throughput rate of the system for the same arrival rate.

Figure 8 shows the curves of throughput rate, collision rate, and idle rate of the channel with arrival rate G for successful time slots taking 1, 2, 5, and 10 time slot lengths at low load with transmit probability $P = 1$. Compared to $P = 0.5$, the throughput rate of the system reaches an inflection point at less than 2, and then the throughput rate basically plateaus as the arrival rate increases.

Combining Figures 6–8, it can be seen that the larger the P value, the faster the throughput rate reaches a relatively stable state when the arrival rate is small, and the different values of P have less impact on the maximum throughput rate. Under the three probability fetches, the maximum throughput rate is about 0.5 for $c = 1$, 0.65 for $c = 2$, 0.82 for $c = 5$, and 0.9 for $c = 10$. Thus, it can be seen that the size of the successful time slot affects the maximum throughput rate of the system in a low competition scenario, and the size of the P value affects the size of the arrival rate corresponding to the maximum throughput rate when the system is fetched.

6.2.2. Experimental Results in a High Competition Scenario (with a Maximum Arrival Rate of 100 to Simulate a High Competition Scenario). The idle time slot length a is taken as 0.1, and the collision time slot length b is taken as 0.5 in the simulation experiment.

Figure 9 shows the curves of throughput rate, collision rate, and idle rate with arrival rate G for channels with successful time slots taken to 1, 2, 5, and 10 time slots length at high load with transmit probability $P = 0.2$. Unlike low load, the throughput rate of the channel starts to show a decreasing trend when the arrival rate reaches above 20, but the throughput rate is still above 0.8 when the success time slot is taken to 10 and at the arrival rate of 100.

Figure 10 shows the curves of throughput rate, collision rate, and idle rate with arrival rate G for channels with successful time slots taken as 1, 2, 5, and 10 time slot lengths for transmit probability $P = 0.5$ under high load. It is clearly seen that the throughput of the channel at $P = 0.5$ drops

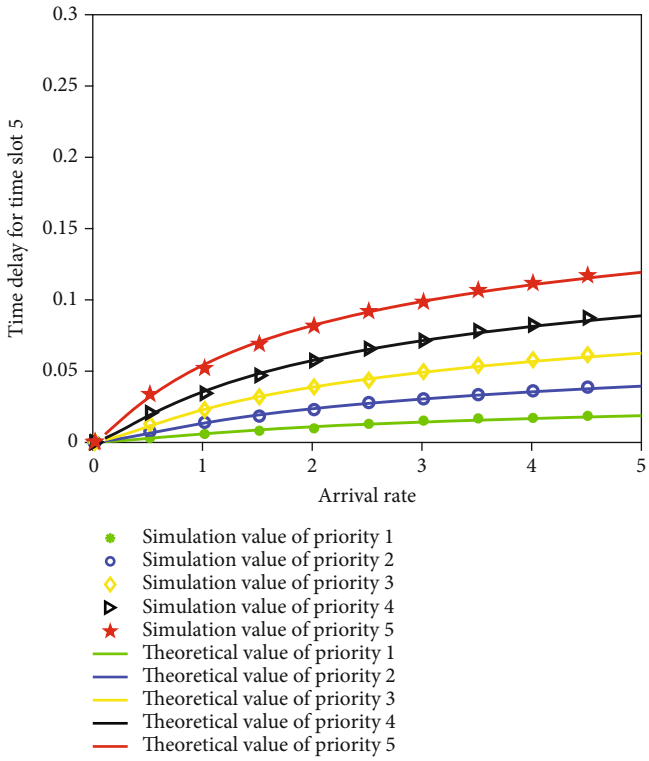

Figure 26: Average delay for $c = 5$ low load multipriority.

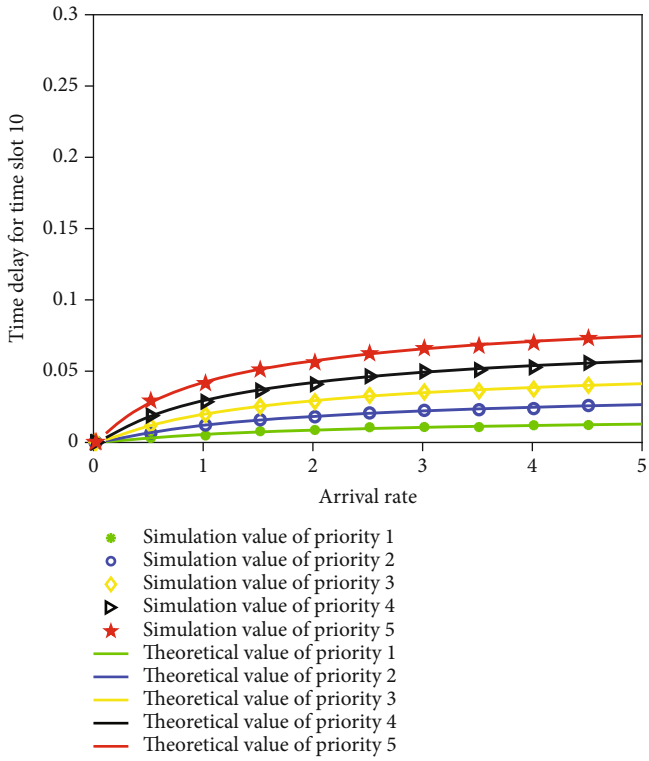

Figure 27: Average delay for $c = 10$ low load multipriority.

sharply after reaching 20, and at an arrival rate of 100, the throughput corresponding to a success time slot taken to 10 is higher than the other values but only close to 0.4.

Figure 11 shows the curves of throughput rate, collision rate, and idle rate with arrival rate G for channels with successful time slots taking 1, 2, 5, and 10 time slot length at high load with transmit probability $P = 1$. It is clearly seen that the throughput rate of the channel at $P = 0.5$ drops sharply after reaching 10, and at an arrival rate of 100, all throughput rates approach 0, regardless of the value of c.

In summary, under high load, regardless of the value of c , the throughput rate is not as good as that under low load when the arrival rate is close to 100, but the throughput rate is also higher under high load when $c = 10$ and $P = 0.2$. Therefore, as long as we ensure that c is relatively large, and P is relatively small, we can ensure that the three-time slot P-CSMA protocol also has better performance under high load.

6.3. Throughput Rate, Collision Rate, and Idle Rate of the System with Multiple Channels and Multiple Priorities

6.3.1. Experimental Results in Low Competition Scenarios. In the simulation experiment, take $a = 0.1$, $b = 0.5$, and $P = 0.2$.

As can be seen in Figures 12–15, the throughput rates for different priority levels increase with increasing arrival rates, regardless of the value of c (the maximum arrival rate is taken to be 10). When c takes the same value, the higher the priority level, the higher the throughput rate of the channel at the same arrival rate; when the priority level is the same, the higher the value of c takes, the higher the throughput rate of the channel at the same arrival rate. Therefore, the higher the value of c, the higher the priority level and the higher the corresponding throughput rate for the same arrival rate.

6.3.2. Experimental Results under High Competition Scenarios. As can be seen in Figures 16–19, the throughput rate of the channel also increases with the arrival rate at high load (the maximum arrival rate is taken as 50). The higher the value of c, the higher the corresponding throughput rate for the same priority level at the same arrival rate. The higher the priority level for the same value of c, the higher the corresponding throughput rate at the same arrival rate.

6.4. Throughput, Collision, and Idle Rates of the System with Different Probabilities. Figure 20 shows the variation curve of the throughput rate with G for the system corresponding to the values of P taken as 0.2, 0.5, 0.8, and 1 for a successful time slot length c of 10. From this figure, it can be seen that the maximum throughput rate of the system is basically the same; the difference is that as P increases, the number of loads G for which the system takes the maximum throughput rate decreases. The reason is that, as P increases, the probability of the system sending information packets directly after they arrive increases, thus increasing the possibility of collision of information packets. So once the maximum throughput rate is reached, the larger G is, the more information packets access the channel at the same time, which means that the more information packets arriv, the more likely collision will occur, then the throughput rate will drop and finally converge to 0.

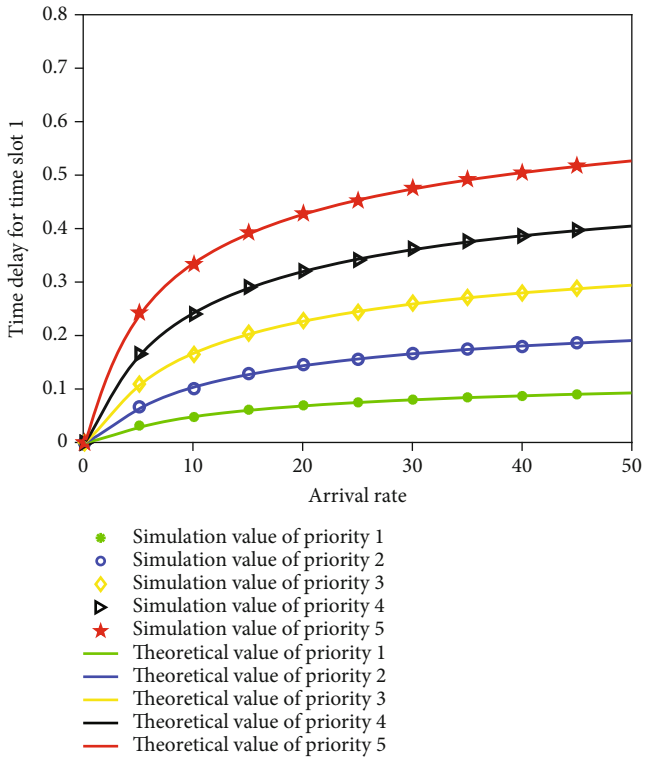

Figure 28: Average delay for $c = 1$ high load multipriority.

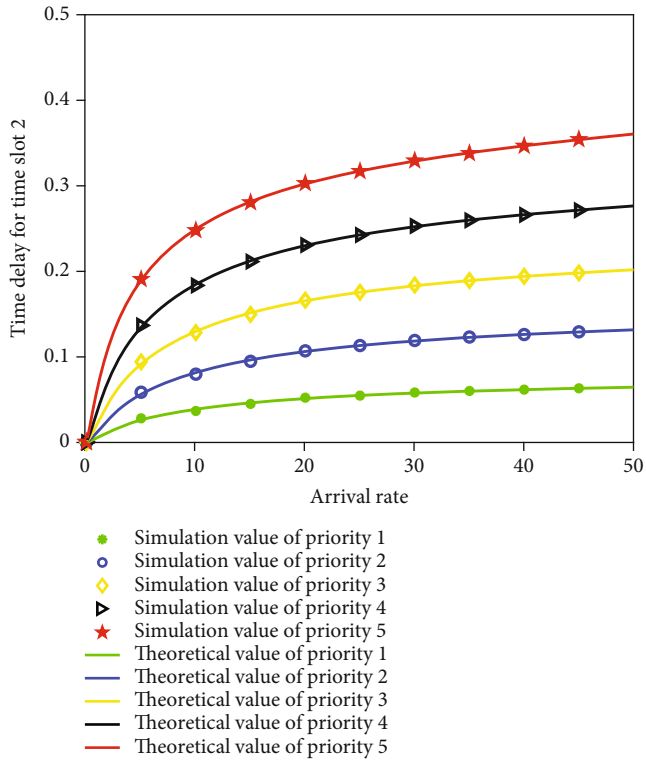

Figure 29: Average delay for $c = 2$ high load multipriority.

6.5. Comparison of System Throughput Rates under Different Protocols. Figure 21 represents the throughput rate of the present improved novel CSMA ($a = 0.5$, $b = 0.1$, $c = 10$, and $P = 0.2$) protocol with nonadherent CSMA ($a = 0.1$, $b = 1$, and $c = 1$) protocol, 1 adherent CSMA ($a = 0.1$, $b = 1$, and $c = 1$) protocol, and P adherent CSMA ($a = 0.1$, $b = 1$, $c = 1$, and $P = 0.2$) protocol with the G curve. From the figure below, it can be seen that the improved CSMA protocol has the highest throughput rate with the same value of G, and the throughput rate is about 0.9 at G of 10; the next highest throughput rate is the nonadherent CSMA, which takes the maximum value of 0.6 at G of 3; the second highest is the 1 adherent CSMA, whose maximum value is about 0.5; the throughput rate of the P adherent CSMA is the worst compared to the other three protocols, whose maximum throughput rate is less than 0.3. In summary, the performance of this new and improved triple-time slot P-CSMA protocol is the best regardless of the value of the load.

6.6. Analysis of Average Time Delay Simulation Experiment Results

6.6.1. Average Delay of a Single Channel. Figures 22 and 23 correspond to the average delay of a single channel under low and high load, respectively. From the above figures, it can be seen that the load is proportional to the delay of the communication channel when c takes the same value, and the higher the load, the higher the channel delay. The reason is that the propagation delay of each information packet in the busy cycle is a, that is, whether the information packet

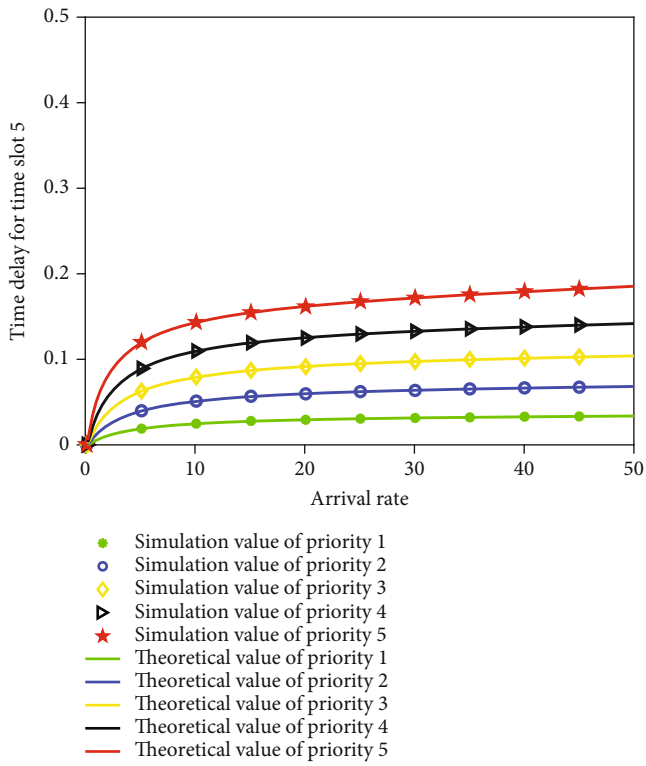

Figure 30: Average delay for $c = 5$ high load multipriority.

is sent successfully or not, there will be a propagation delay of a after arriving at the channel, so the more information packets are sent, the corresponding channel delay will be

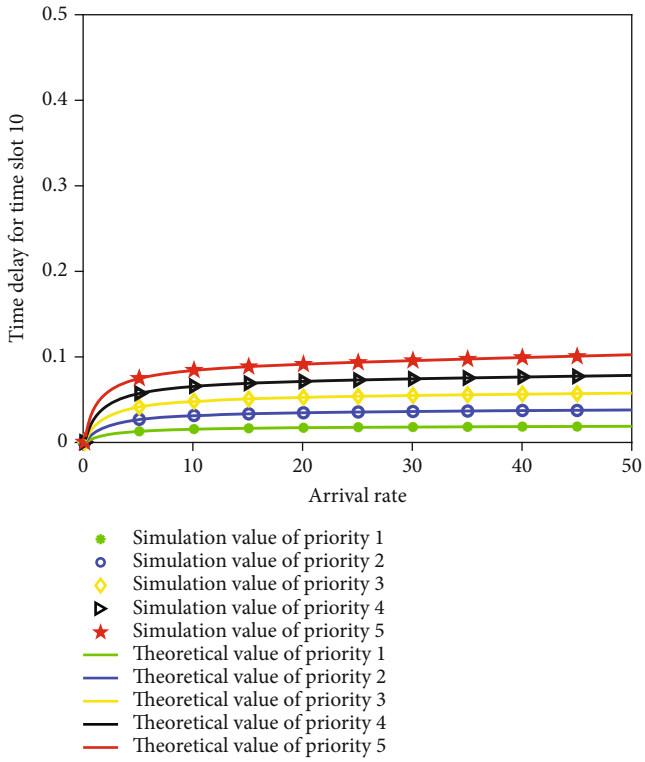

Figure 31: Average delay for $c = 10$ high load multipriority.

larger. Among them, the larger the value of the success time slot c is, the smaller the average delay of the channel will be for the same arrival rate. Because, the larger the value of c, the longer a transmission period Tn, the average delay of the channel will be reduced if the transmission delay of each message packet remains unchanged.

6.6.2. Average Delay of Multiple Channels. As can be seen from Figures 24–27, when c takes the same value, at the same arrival rate, the higher the priority level, the higher the average delay of the channel, and the average delay of the channel increases with the arrival rate; at the same priority level, at the same arrival rate, the larger the value of c takes, the smaller the average delay of the channel. Because the higher the priority level, the more the number of channels occupied by the sending packet, there will be a delay of size a in each channel for the sending packet, so the higher the number of channels, the higher the average delay of the channel. In addition, as with single channel, the larger the value of c is taken, the larger the transmission period Tn is, and the larger the c is, the smaller the average delay is under sending the same message packet.

Figures 28–31 correspond to the average delay of the channel under high load when c takes different values.

As in the case under low load, the higher the c, the lower the priority and the lower the average delay of the channel for the same arrival rate. The average delay of the channel is proportional to the arrival rate of the message packet, i.e., the higher the arrival rate, the higher the average delay of the channel.

7. Conclusion

The main contribution of this paper is to propose a new communication protocol model. In the edge server network, for the problem that the traditional CSMA protocol does not have a high throughput rate under high load, this paper proposes a three-time slot P-insistence CSMA protocol with multiple priorities and variable success time. Through simulation experiments, it can be seen that the longer the success time, the lower the probability of sending and the less the possibility of collision of message packets, and thus the higher the throughput rate of the system under high load, with constant idle time and collision time. Under the multiuser multiedge server condition, the higher the priority level of the user, the more edge servers are occupied, and the user's information can be sent successfully even under high load relatively easily. Finally, the new P-CSMA protocol ($C = 10$; $P = 0.2$) proposed in this paper is compared with other protocols, and the experimental results show that the throughput rate of this protocol is always higher than other protocols, and it also has better performance at higher loads. We expect that this protocol provides a better solution for improving the throughput performance of an edge server network used by multiple users.

Data Availability

The data for the article is available and I will open source the data for the paper when the article is published.

Conflicts of Interest

The authors declare that they have no conflicts of interest.

Acknowledgments

This work was supported by the Opening Foundation of Yunnan Key Laboratory of Smart City in Cyberspace Security (No. 202105AG070010) and National Natural Science Foundation of China, Research on Theory and Control Protocol of Converged Multiple Access Communication Network (No. 61461053).

References

[1] F. Bonomi, R. Milito, J. Zhu, and S. Addepalli, "Fog computing and its role in the internet of things," in *Proceedings of the first edition of the MCC workshop on Mobile cloud computing*, pp. 13–16, Helsinki, Finland, 2012.

[2] Y. H. Bae, B. D. Choi, and A. S. Alfa, "Achieving maximum throughput in random access protocols with multipacket reception," *IEEE Transactions on Mobile Computing*, vol. 13, no. 3, pp. 497–511, 2014.

[3] R. Rom and M. Sidi, *Multiple Access Protocols: Performance and Analysis, [M.S. thesis]*, Springer Science & Business Media, 2012.

[4] S. C. Ergen and P. Varaiya, "TDMA scheduling algorithms for wireless sensor networks," *Wireless Networks*, vol. 16, no. 4, pp. 985–997, 2010.

[5] A. Sgora, D. J. Vergados, and D. D. Vergados, "A survey of TDMA scheduling schemes in wireless multihop networks," *ACM Computing Surveys (CSUR)*, vol. 47, no. 3, pp. 1–39, 2015.

[6] Z. Chen, Y. Liu, R. Liu, J. Yuan, and D. Han, "Improved CSMA/CA algorithm based on alternative channel of power line and wireless and first-time idle first acquisition," *IEEE Access*, vol. 7, pp. 41380–41394, 2019.

[7] D. N. M. Dang and C. S. Hong, "H-MMAC: a hybrid multi-channel MAC protocol for wireless ad hoc networks," in *2012 IEEE international conference on communications (ICC)*, pp. 6489–6493, Ottawa, ON, Canada, 2012.

[8] S.-L. Wu, C.-Y. Lin, Y.-C. Tseng, and J.-L. Sheu, "Anew multi-channel MAC protocol with on-demand channel assignment for multi-hop mobile ad hoc networks," in *Proceedings International Symposium on Parallel Architectures, Algorithms and Networks. I-SPAN 2000*, pp. 232–237, Dallas, TX, USA, 2000.

[9] J. So and N. H. Vaidya, "Multi-channel MAC for ad hoc networks: handling multi-channel hidden terminals using a single transceiver," in *Proceedings of the 5th ACM International Symposium on Mobile Ad Hoc Networking and Computing (Mobihoc'04)*, pp. 222–233, Roppongi Hills, Tokyo, Japan, 2004.

[10] K.-P. Shih, Y.-D. Chen, and S.-S. Liu, "A collision avoidance multi-channel MAC protocol with physical carrier sensing for mobile ad hoc networks," in *IEEE 24th International Conference on Advanced Information Networking and Applications Workshops (WAINA)*, pp. 656–661, Perth, WA, Australia, 2010.

[11] D. N. M. Dang, C. S. Hong, S. Lee, and J. Lee, "A sinr-based mac protocol for wireless ad hoc networks," *IEEE Communications Letters*, vol. 16, no. 12, pp. 2016–2019, 2012.

[12] N. H. Tran and C. S. Hong, "Joint rate and power control in wireless network: a novel successive approximations method," *IEEE Communications Letters*, vol. 14, no. 9, pp. 872–874, 2010.

[13] N. H. Tran, C. S. Hong, and S. Lee, "Joint congestion control and power control with outage constraint in wireless multihop networks," *IEEE Transactions on Vehicular Technology*, vol. 61, no. 2, pp. 889–894, 2012.

[14] L. Mingliang, D. Hongwei, L. Bo, B. Liyong, and H. Li, "Analysis of three-time slot 1P-CSMA protocol with variable collision duration in WSN," *Modern Electronics Technology*, vol. 44, no. 9, pp. 12–18, 2021.

[15] L. Mingliang, D. Hongwei, L. Bo, W. Liqing, and B. Liyong, "Analysis of three-time slot P-adherent CSMA protocol with variable collision duration in WSN," *Computer Applications*, vol. 40, no. 7, pp. 2038–2045, 2020.

[16] H. Ze-jun, D. Hongwei, Y. Kun, L. Chunfen, and Y. Zhijun, "Analysis of WSN protocols with three-clock N-CSMA with variable collision length," *Journal of Yunnan University (Natural Science Edition)*, vol. 41, no. 4, pp. 699–706, 2019.

[17] S. J. Zhou, H. W. Ding, C. J. Yang, and L. Pianlin, "Research on adaptive 3D probabilistic CSMA control strategy," *Journal of Electronics*, vol. 45, no. 2, pp. 440–445, 2017.

[18] M. V. S. Alves and J. C. Basilio, "State estimation and detectability of networked discrete event systems with multi-channel communication networks," *IEEE Transactions on Automation Science and Engineering*, pp. 1–16, 2023.

[19] F. Ali, S. Ahmad, F. Muhammad, Z. H. Abbas, U. Habib, and S. Kim, "Adaptive equalization for dispersion mitigation in multi-channel optical communication networks," *Electronics*, vol. 8, no. 11, p. 1364, 2019.

[20] J. Xu, C. Luo, G. Parr, and Y. Luo, "A spatiotemporal multi-channel learning framework for automatic modulation recognition," *IEEE Wireless Communications Letters*, vol. 9, no. 10, pp. 1629–1632, 2020.